IEEE Access
Multidisciplinary | Rapid Review | Open Access Journal

Received July 4, 2017, accepted August 14, 2017, date of publication August 17, 2017, date of current version September 19, 2017.

Digital Object Identifier 10.1109/ACCESS.2017.2740938

Consensus of Teleoperating Cyber-Physical System via Centralized and Decentralized Controllers

JING YAN[1], XIAN YANG[2], XIAOYUAN LUO[1], CAILIAN CHEN[3], AND XINPING GUAN[3]

[1]Department of Automation, Yanshan University, Qinhuangdao 066004, China
[2]Institute of Information Science and Engineering, Yanshan University, Qinhuangdao 066004, China
[3]Department of Automation, Shanghai Jiao Tong University, Shanghai 200240, China

Corresponding author: Jing Yan (jyan@ysu.edu.cn)

This work was supported in part by NSF of China under Grant 61503320, Grant 61375105, and Grant 61603328, in part by the China Postdoctoral Science Foundation under Grant 2015M570235, Grant 2017T100166, Grant 2016M600195, and Grant 2016T90214, in part by NSF of Hebei Province under Grant F2016203117, in part by Educational Committee Foundation of Hebei Province under Grant QN2015187, in part by the Hebei Postdoctoral Science Foundation under Grant F2016203311 and Grant B2015003018, in part by the Open Project Programs of the Key Laboratory of System Control and Information Processing Ministry of Education under Grant Scip201501, and in part by Yanshan University under Grant 14LGA010 and Grant B2015003018.

ABSTRACT Teleoperating cyber-physical system (TCPS) has been considered as a promising technology to stretch artificial intelligences to remote locations. Many applications of TCPS demand operator and slaves to keep state consensus on the shared information. However, the cyber- and physical- constrained characteristics on TCPS make it difficult to realize such a consensus. This paper investigates the consensus problem for single-master-multi-slave TCPS with time-varying delay and actuator saturation. According to the communication structures of slaves, centralized and decentralized controllers are, respectively, designed to drive the consensus of master and slave robots. To simplify the information fusion in decentralized controller design, we use min-weighted rigid graph-based topology optimization algorithm to reduce the communication redundancy in slave site. Under time-varying delay and actuator saturation constraints, the sufficient stability conditions are presented to show that the centralized and decentralized controllers can stabilize the single-master-multi-slave TCPS. Moreover, the stability conditions are rearranged into a form of linear matrix inequalities, and then, the required initial stability conditions for master and slaves are developed. Finally, simulations and experiments are demonstrated to show the validity of the method. It is shown that the consensus controllers can guarantee the asymptotic stability of single-master-multi-slave TCPS, while the topology optimization can reduce the redundancy of communication links.

INDEX TERMS Consensus, cyber-physical system (CPS), teleoperation, time delay.

I. INTRODUCTION

With the advent of artificial intelligent technology, autonomous physical devices have increasingly been used as flexible sensing and computational platforms for a variety of applications, such as AlphaGo game, port surveillance, environment monitoring, disaster prevention and blind navigation in unknown environments; see [1]–[3] and the references. However, in some dangerous and dynamic scenarios (e.g., neutron monitoring for nuclear power industry), pure autonomy operation is not adequate for physical devices to achieve complicated missions. In such scenarios, it becomes favorable for multiple physical devices to cooperatively achieve the tasks assisted by human operators. Teleoperating cyber-physical system (TCPS), which is usually operated in a master–slave configuration, stretches artificial intelligences to remote locations and allows human to concentrate on high-level reasoning and decision making.An illustration of TCPS is shown in Fig. 1. The application of TCPS includes multiple fields, e.g., space and deep sea exploiting systems, telemedicine and robot-assisted surgery systems, hazardous environment monitoring and rescue applications [4].

One important issue for TCPS is to design appropriate controllers such that the group of physical devices can achieve state *consensus* on the shared information. Recent studies show that consensus capacitates numerous applications in conventional research areas, e.g., flocking and formation

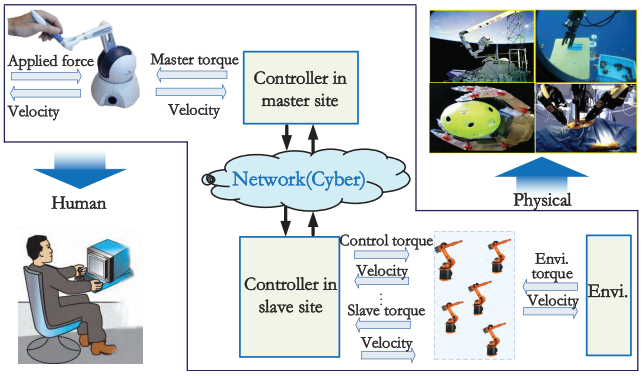

FIGURE 1. A standard collaborative relationship for TCPS.

control in multi-agent systems [5], as well as other newly emerging systems, for example, scheduling and optimization in wireless networks [6], economic dispatch in smart grid [7], privacy-preserving data aggregation [8], and so on. In TCPS, *consensus* means that the states of master and slave physical devices (i.e., robots) converge to the same state value. To address this problem, consensus-based tracking controllers for master and slaves were designed in [9] and [10]. However, the influence of time delay between human operator and slaves is not considered. For a remote controlled TCPS, time delays associated with propagation are inevitable to a certain extent. Although some literatures have given time-delay based controllers for teleoperation system [11], the proposed controllers cannot be directly adopted to solve the consensus problem for multi-slave TCPS due to the single-slave configuration. For seeking the cooperation of physical devices, a multi-slave configuration is preferred for TCPS. In multi-slave configuration setting, a consensus-based state convergence problem was investigated in [12], however the time delays in communication channel are ignored. In [13], a consensus-based formation controller was given to plan the trajectories of master and slaves, where the time delays in communication channel are assumed to be constant. In order to better capture the cyber-constrained characteristics, time-varying delays of TCPS are preferred. Moreover, in almost all control systems including TCPS, the physical devices are inherently limited by the physical nature of devices, i.e., the existence of actuator saturation. If actuator saturation is ignored, undesirable responses and even instability can occur [14]. Therefore, it is highly appreciate to take the time-varying delays and actuator saturation into the controller design process. Inspired by this, some methods have been proposed, for example [15]–[17] and the references therein. Nevertheless, the physical devices in the above literatures are single-master configurations, which cannot be directly applied to multi-slave TCPS. Also of relevance, our previous works [18]–[20] have investigated the formation control for single-master-multi-slave TCPS. However, with time delay and actuator saturation constraints, how to design a consensus controller to stabilize the TCPS is still not well addressed.

On the other hand, effective communication of master and slaves is critical for the achievement of consensus, especially when the communication channel and transmission power are limited. Normally, the communication structures can be classified into centralized and decentralized ones. Centralized structures (i.e., all slaves communicate with a single master [13], [21]–[23]) are effective with the minimum number of data transmission, however they are not practical in large-scale networks due to a variety of issues, e.g., the vulnerability to attacks, data traffic bottlenecks, and lack of flexibility, and the incapability to scale. In contrast, decentralized structures (i.e., neighbor rule is adopted to demonstrate the topology of master and slaves [18], [24]) achieve better performance on security, throughput, flexibility and scalability. By analyzing the neighbor rule-based topology relationship of slave robots, it reveals that some interactions are unnecessary. This drawback makes the communication in slave site complex and inefficient. In our previous work [19], we design a rigid graph-based optimization scheme to save the communication consumption in slave site. Nevertheless, it is still unknown whether the rigid graph-based optimization scheme can improve the consensus performance in multi-slave TCPS.

In this paper, we are concerned with a consensus problem for multi-slave TCPS with time delay and actuator saturation constraints. As shown in Fig. 1, master obtains the desired trajectory through human operator. The position and velocity signals are then sent to the slaves so that the slaves can track the motion of master. It is not a simple task of consensus tracking because the effect of environment force is also transmitted back to the master site so that the human operator can feel the presence of the remote environment. Main contributions of this paper are summarized as follows.

- A centralized controller is designed to enforce the consensus of master and slaves, and the sufficient stability conditions are given to show that the centralized controller can stabilize the master-slave TCPS. Compared with [13], [22], time-varying delay and actuator saturation are both incorporated in the controller design.
- To simplify the information fusion, a rigid graph based topology optimization scheme is given to reduce the redundancy of communication links. Then, a decentralized consensus controller is designed while the sufficient stability conditions are also presented.
- Rearrange the stability conditions into the form of linear matrix inequalities (LMIs), and then we estimate the domain of attraction (DOA). Based on this, the required initial stability conditions for TCPS can be obtained, such that master and slave robots can adjust the initial states to guarantee the consensus stability.

Notation: $\mathcal{R}^n$ denotes the n-dimensional Euclidean space, $\mathcal{R}^{n\times n}$ denotes the set of $n \times n$ real matrices, I represents the identity matrix, $|\cdot|$ denotes the absolute of a parameter, "$*$" denotes an ellipsis for the terms by symmetry, and superscript "T" is for matrix transposition. $\mathrm{col}(x_1, \cdots, x_n)$ represents a column vector by stacking column vectors $x_1, \cdots, x_n$

together. $X > 0$ means X is real symmetric positive definite.

II. PROBLEM FORMULATION

A. DYNAMIC MODEL OF MASTER AND SLAVE ROBOTS

In this paper, the TCPS is composed of a single n-degree-of-freedom (DOF) master robot and N n-DOF slave robots. The dynamics of master and slave robots are shown as

$$\begin{aligned} M_m(q_m)\ddot{q}_m + C_m(q_m)\dot{q}_m + G_m(q_m) &= F_h - S(\tau_m) \\ M_1(q_1)\ddot{q}_1 + C_1(q_1)\dot{q}_1 + G_1(q_1) &= S(\tau_1) + F_{e1} \\ \vdots \qquad & \vdots \\ M_N(q_N)\ddot{q}_N + C_N(q_N)\dot{q}_N + G_N(q_N) &= S(\tau_N) + F_{eN} \end{aligned} \quad (1)$$

where q_i, $\dot{q}_i$, $\ddot{q}_i \in \mathcal{R}^n$ are respectively the joint displacement, velocity and acceleration. $M_i(q_i)$ is the inertia matrix, $C_i(q_i, \dot{q}_i)$ is the centrifugal and Coriolis matrix, $G_i(q_i) \in \mathcal{R}^n$ represents the gravitational torque, and $F_h \in \mathcal{R}^n$ and $F_i \in \mathcal{R}^n$ are the human-operator force (torque) and environment force (torque), respectively. $\tau_i \in \mathcal{R}^n$ is the control torque restricted by a given saturation bound $T = [T_1, \cdots, T_n]^T$, i.e., each element τ_{ir} of τ_i satisfies $|\tau_{ir}| \le T_r$ where $T_r > 0$ and $r = 1, \cdots, n$. In addition, $i = m$ denotes the master robot, and $i = 1, \cdots, N$ denotes the i th slave robot.

The system (1) has the following properties [25].

Property 1: Inertia matrix is bounded, i.e., for $\check{\varrho}_i, \hat{\varrho}_i \in \mathcal{R}^+$

$$0 < \check{\varrho}_i I \le M_i(q_i) \le \hat{\varrho}_i I < \infty. \quad (2)$$

Property 2: Matrix $\dot{M}_i(q_i) - 2C_i(q_i, \dot{q}_i)$ is skew-symmetric.

Property 3: For a manipulator with revolute joints, the gravity vector $G_i(q_i)$ is bounded, i.e., there exist positive constants ϑ_r such that every element of the gravity vector, $G_{ir}(q_i)$, $r = 1, \cdots, n$, satisfies $|G_{ir}(q)| < \vartheta_r$.

In this paper, time delay from slave i to master can be denoted as $d_{im}(t)$, while the time delay from master to slave i can be denoted as $d_{mi}(t)$. For stability analysis, we give the following assumptions and lemmas.

Assumption 1: In this paper, $d_{im}(t)$ and $d_{mi}(t)$ are both lower and upper bounded, and there exist positive scalars $\check{d}_{sm}$, $\hat{d}_{sm}$, $\check{\mu}_{sm}$, $\hat{\mu}_{sm}$, $\check{d}_{ms}$, $\hat{d}_{ms}$, $\check{\mu}_{ms}$ and $\hat{\mu}_{ms}$ such that $\check{d}_{sm} \le d_{im}(t) \le \hat{d}_{sm} < \infty$, $\check{\mu}_{sm} \le \dot{d}_{im}(t) \le \hat{\mu}_{sm}$, $\check{d}_{ms} \le d_{mi}(t) \le \hat{d}_{ms} < \infty$ and $\check{\mu}_{ms} \le \dot{d}_{mi}(t) \le \hat{\mu}_{ms}$ for $\forall i = 1, \cdots, N$. In addition, it is assumed that $\check{d}_i = \check{d}_{sm} + \check{d}_{ms}$, $\hat{d}_i = \hat{d}_{sm} + \hat{d}_{ms}$, $d_i(t) = d_{im}(t) + d_{mi}(t)$, $\check{\mu}_i = \check{\mu}_{sm} + \check{\mu}_{ms} < 1$, $\hat{\mu}_i = \hat{\mu}_{sm} + \hat{\mu}_{ms} < 1$, and $d_2 = \max\{\hat{d}_{sm}, \hat{d}_{ms}\}$.

Assumption 2: Human operator and the environment in this paper are passive, i.e., for non-redundant manipulator,

$$\int_0^t \dot{q}_m^T(\sigma)F_h(\sigma)d\sigma \ge 0, \quad \int_0^t -\dot{q}_i^T(\sigma)F_i(\sigma)d\sigma \ge 0. \quad (3)$$

Lemma 1 [14]: Given feedback matrices K, H, if the state vector x satisfies $|h_j x| \le M_{\max,j}$, then

$$\text{sat}(Kx) \in \text{co}\{D_i Kx + D_i^- Hx, i = 1, \ldots .2^n\}$$

where h_j is the jth row of H for all $j = 1, \ldots, n$, $\text{sat}(\cdot)$ denotes the saturation function with level $M_{\max}$, and $\text{co}\{\cdot\}$ is the convex hull of a set. D denotes the set of $n \times n$ diagonal matrices D_i with 0 or 1 as its diagonal entries, i.e., $D = \{D_i : i = 1, \cdots, 2^n\}$ and $D_i^- = I - D_i$.

Lemma 2 [26]: Define $l_U(\omega) = \int_a^b \omega^T(u)U\omega(u)du$ for a given matrix $U > 0$, then the following inequality holds for all continuously differentiable function ω in $[a, b] \to \mathcal{R}^n$:

$$l_U(\dot{\omega}) \ge \frac{1}{b-a}(\omega(b) - \omega(a))^T U(\omega(b) - \omega(a)) + \frac{3}{b-a}\tilde{\Omega}^T U\tilde{\Omega},$$

where $\tilde{\Omega} = \omega(b) + \omega(a) - \frac{2}{b-a}\int_a^b \omega(u)du$.

The following example is given to explain Lemma 1.

Example 1: Since $|h_j x| \le M_{\max,j}$, we have $\text{sat}(k_j x) \in \text{co}\{k_j x, h_j x\}$, where k_j denotes the j th row of K for all $j = 1, \ldots, n$. If $n = 1$, $\text{sat}(k_1 x) = \alpha_1 k_1 x + \alpha_2 h_1 x$ where $\alpha_1 + \alpha_2 = 1$, i.e., $\text{sat}(k_1 x) \in \text{co}\{k_1 x, h_1 x\}$. If $n = 2$, $\text{sat}\left(\begin{bmatrix} k_1 x \\ k_2 x \end{bmatrix}\right) = \begin{bmatrix} \alpha_1(\beta_1 + \beta_2)k_1 x + \alpha_2(\beta_1 + \beta_2)h_1 x \\ \beta_1(\alpha_1 + \alpha_2)k_2 x + \beta_2(\alpha_1 + \alpha_2)h_2 x \end{bmatrix} = \alpha_1\beta_1 \times \begin{bmatrix} k_1 x \\ k_2 x \end{bmatrix} + \alpha_1\beta_2 \begin{bmatrix} k_1 x \\ h_2 x \end{bmatrix} + \alpha_2\beta_1 \begin{bmatrix} h_1 x \\ k_2 x \end{bmatrix} + \alpha_2\beta_2 \begin{bmatrix} h_1 x \\ h_2 x \end{bmatrix}$. As $\beta_1 + \beta_2 = 1$ and $\sum_{i=1}^{2}\sum_{j=1}^{2} \alpha_i\beta_j = 1$, we have $\text{sat}\left(\begin{bmatrix} k_1 x \\ k_2 x \end{bmatrix}\right) \in \text{co}\left\{\begin{bmatrix} k_1 x \\ k_2 x \end{bmatrix}, \begin{bmatrix} k_1 x \\ h_2 x \end{bmatrix}, \begin{bmatrix} h_1 x \\ k_2 x \end{bmatrix}, \begin{bmatrix} h_1 x \\ h_2 x \end{bmatrix}\right\}$. If $n = 3$, $\text{sat}\left(\begin{bmatrix} k_1 x \\ k_2 x \\ k_3 x \end{bmatrix}\right) \in \text{co}\left\{\begin{bmatrix} k_1 x \\ k_2 x \\ k_3 x \end{bmatrix}, \begin{bmatrix} k_1 x \\ k_2 x \\ h_3 x \end{bmatrix}, \begin{bmatrix} k_1 x \\ h_2 x \\ k_3 x \end{bmatrix}, \begin{bmatrix} k_1 x \\ h_2 x \\ h_3 x \end{bmatrix}, \begin{bmatrix} h_1 x \\ k_2 x \\ k_3 x \end{bmatrix}, \begin{bmatrix} h_1 x \\ k_2 x \\ h_3 x \end{bmatrix}, \begin{bmatrix} h_1 x \\ h_2 x \\ k_3 x \end{bmatrix}, \begin{bmatrix} h_1 x \\ h_2 x \\ h_3 x \end{bmatrix}\right\}$. Finally, one obtains $\text{sat}(Kx) \in \text{co}\{D_i Kx + D_i^- Hx, i = 1, \ldots .2^n\}$. Then, $\text{sat}(Kx)$ is refreshed as $\text{sat}(Kx) = \sum_i^{2^n} \eta_i(D_i Kx + D_i^- Hx)$, where $0 \le \eta_i \le 1$, $\sum_{i=1}^{2^n} \eta_i = 1$. Specially, Fig. 2(a) is given to illustrate Lemma 1.

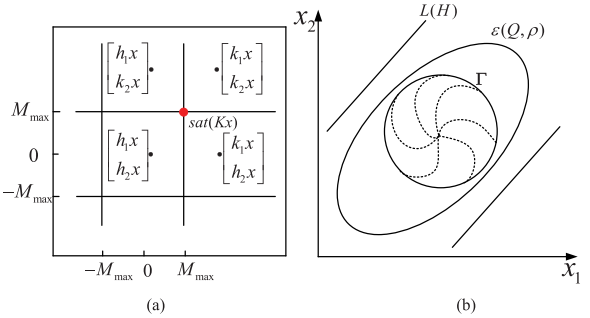

FIGURE 2. (a) Illustration for Lemma 1 where $n = 2$. (b) Relationship of $L(H)$, $\varepsilon(Q, \rho)$ and the DOA where $M_{\max,j} = M_{\max}$.

For initial state vector $x(0) = x_0$, the state trajectory is denoted as $\psi(t, x_0)$, and the DOA of the origin is $\Gamma = \{x_0 : \lim_{t\to\infty} \psi(t, x_0) = 0\}$. A set is said to be *invariant* if all trajectories starting from the DOA will remain in it. With Lemma 1, we can place $\text{sat}(Kx)$ into the convex hull of a group of linear feedbacks under the condition of $L(H) = \{x : |h_j x| \le M_{\max,j}\}$ where $j = 1, \ldots, n$. Notice that a subset

of the set $L(H)$ is chosen to be an ellipsoid with the form $\varepsilon(Q,\rho) = \{x : x^T Q x \leq \rho\}$, where $Q > 0$ and $\rho \in \mathcal{R}^+$. Therefore, if $\varepsilon(Q,\rho)$ is contractively invariant, it is inside the DOA. If $n = 2$, the relationship among $L(H)$, $\varepsilon(Q,\rho)$ and the DOA is illustrated in Fig. 2 (b). In this paper, we attempt to develop conditions under which $\varepsilon(Q,\rho)$ is contractively invariant, and thus an estimate of the DOA can be obtained.

B. TOPOLOGY RELATIONSHIP OF MASTER AND SLAVES

In order to achieve state consensus, this paper attempts to design centralized and decentralized controllers for TCPS. In centralized controller, each slave bilaterally communicates with the master. Alternatively, decentralized controller relies on neighbor rule to describe the topology relationship of master and slaves, where each slave only communicates with the slaves in its neighborhood. To reduce the redundancy of communication links in slave site, the neighbor rule-based topology relationship can be optimized by a rigid graph. Inspired by this, some basic concepts of rigid graph are introduced [27].

A *graph* $\mathcal{G}$ is a pair of vertices $\mathcal{V} = \{1,\ldots,N\}$ and edges $\mathcal{E} \subseteq \mathcal{V} \times \mathcal{V}$. The graph is said to be *undirected* if $(i,j) \in \mathcal{E}$ and $(j,i) \in \mathcal{E}$. The number of vertices in $\mathcal{V}$ is shown as $|\mathcal{V}|_{\#}$, while the number of edges in $\mathcal{E}$ is $|\mathcal{E}|_{\#}$. An edge denoted as (j,i) means that node i can receive the information from node j. For slave robot i ($i = 1,\cdots,N$), sensing sensor is mounted at the base of the manipulator, and the position of this sensor is denoted by $p_i \in \mathcal{R}^3$. The neighbor set of sensor i is denoted by $\Im_i = \{j \in \mathcal{V}: \|p_i - p_j\| \leq \vec{r}, j \neq i\}$, where $\vec{r} > 0$ is the sensing range. When sensor j is a neighbor of sensor i, it means that slave robot i can communicate with slave robot j. Based on this, the *adjacency matrix* $\mathcal{A} = [a_{ij}] \in \mathcal{R}^{N\times N}$ is defined, where $a_{ij} > 0$ if $j \in \Im_i$ and $a_{ij} = 0$ otherwise. With connectivity maintenance, we assume the master robot can always transmit and access the state information of one slave robot, and the graph describing the information structure of salvers is assumed to be connected, where a graph is *connected* if any two vertices can be joined with a path.

Given a graph $\mathcal{G} = (\mathcal{V},\mathcal{E})$ with N vertices, positions $p_i \in \Re^3$ and $i \in \mathcal{V}$, if $\forall (i,j) \in \mathcal{E}$ satisfies $||p_i - p_j|| = \Upsilon > 0$, and $(p_i - p_j)^T(\dot{p}_i - \dot{p}_j) = 0$ at the initial rotation time, $\dot{p} = (\dot{p}_1, \dot{p}_2, \ldots, \dot{p}_N)$ is called as an *infinitesimal flex*. A graph is *infinitesimally rigid graph* if it only has trivial infinitesimal flex. The detailed definition of the concept of *infinitesimal rigidity* is presented in [28]. Correspondingly, the rigidity matrix $R(\mathcal{G})$ is defined as the $|\mathcal{E}|_{\#} \times 3|\mathcal{V}|_{\#}$ matrix, i.e.,

$$\begin{bmatrix} \vdots & \ddots & \vdots & & \vdots & \cdots & \vdots & & \vdots & \ddots & \vdots \\ 0 & \cdots & 0 & p_i^T - p_j^T & 0 & \cdots & 0 & p_j^T - p_i^T & 0 & \cdots & 0 \\ \vdots & \ddots & \vdots & & \vdots & \cdots & \vdots & & \vdots & \ddots & \vdots \end{bmatrix},$$

where each row $\begin{bmatrix} 0 \cdots 0 & p_i^T - p_j^T & 0 \cdots 0 & p_j^T - p_i^T & 0 \cdots 0 \end{bmatrix}$ corresponds to an edge $(i,j) \in \mathcal{E}$, $p_i^T - p_j^T$ is a row 3-vector in the three columns corresponding to node i.

All infinitesimally rigid networks are rigid, and infinitesimal rigidity of a graph is a stronger condition than rigidity. The following proposition is given to show the relationship between infinitesimally rigid graph and rigidity matrix.

Proposition 1: A graph with $N > 3$ vertices in $\mathcal{R}^3$ is infinitesimally rigid if and only if $\text{rank}(R(\mathcal{G})) = 3N - 6$. An infinitesimally rigid graph $\mathcal{G} = (\mathcal{V},\mathcal{E})$ with $N > 3$ vertices and $3N - 6$ edges is *minimally rigid*. If every edge of the graph $\mathcal{G} = (\mathcal{V},\mathcal{E})$ is weighted by its length, a *min-weighted rigid graph* is the minimally rigid graph which has the minimally weighted sum in all infinitesimally rigid graphs.

C. PROBLEM FORMULATION

Two problems are considered in this paper, centralized consensus controller design and rigid graph-based decentralized consensus controller design.

Problem 1 (Centralized Consensus Controller Design): In order to achieve state consensus, we attempt to design a centralized consensus controller and give the stability conditions, whose DOA is estimated to guarantee the state consensus.

Problem 2 (Rigid Graph-Based Decentralized Consensus Controller Design): To improve the flexility and scalability, we attempt to design a decentralized consensus controller while the stability conditions and DOA are also given. Moreover, a rigid graph based topology optimization scheme is provided to reduce the redundancy of communication links.

III. MAIN RESULT

In this section, we detail the consensus controller design process. We first design a centralized consensus controller to enforce the state consensus of master and slaves. Then, a decentralized consensus controller is designed, while a rigid graph based topology optimization scheme is given to reduce the redundancy of communication links.

A. DESIGN OF CENTRALIZED CONSENSUS CONTROLLER

Under centralized network topology, master robot tracks the geometric center of slave robots, i.e., $q_m \to \frac{1}{N}\sum_{i=1}^{N} q_i$, and slave robots move as a group along the states enforced by the master robot, i.e., $q_i \to q_m$. Then, the centralized consensus controller for master and slave robot i ($\forall i = 1,\cdots,N$) is designed as

$$\begin{aligned} \tau_m &= \text{sat}(K_m(\frac{1}{N}\sum\nolimits_{i=1}^{N} q_i(t - d_{im}) - q_m) - \alpha_m \dot{q}_m) \\ &\quad + G_m(q_m) \\ \tau_i &= \text{sat}(K_i(q_m(t - d_{mi}) - q_i) - \alpha_i \dot{q}_i) + G_i(q_i) \end{aligned} \tag{4}$$

where K_m, α_m, K_i, $\alpha_i \in \mathcal{R}^{n\times n}$ are gain matrices. With Property 3, one obtains that $|G_{ir}(q)| < \vartheta_r$ for $\forall r = 1,\ldots,n$. Then, the rth element $M_{\max,r}$ of $M_{\max}$ satisfies $M_{\max,r} \leq T_r - \vartheta_r$. The control framework is shown in Fig. 3.

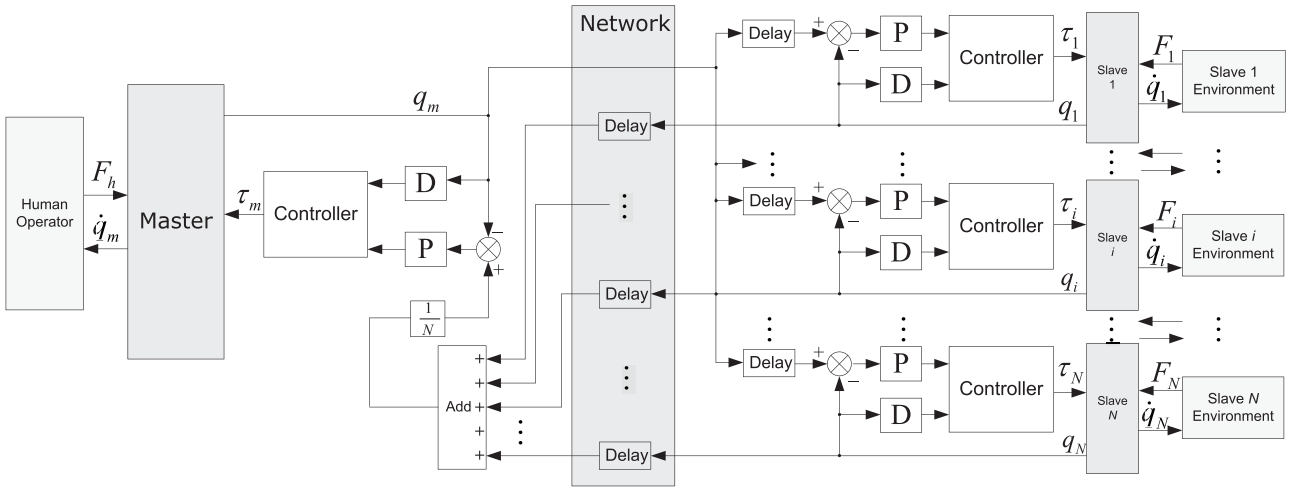

FIGURE 3. Control framework of the centralized consensus controller.

To demonstrate the DOA, bounds of the initial values are defined as

$$\begin{aligned}
\max_{\theta\in[-d_2,0]} \|\dot{q}_{m0}(\theta)\| &\le \delta_{m1},\\
\max_{\theta\in[-d_2,0]} \|\dot{q}_{sr0}(\theta)\| &\le \delta_{sr1},\\
\max_{\theta\in[-d_2,0]} \|q_{m0}(\theta) - q_{sr0}(\theta)\| &\le \delta_{er1},\\
\max_{\theta\in[-d_2,0]} \|\dot{q}_{m0}(\theta) - \dot{q}_{sr0}(\theta)\| &\le \delta_{er2}, \quad r = 1, 2, \ldots, N \qquad (5)
\end{aligned}$$

where δ_{m1}, δ_{sr1}, δ_{er1} and δ_{er2} are positive parameters.

Remark 1: As the relative distances between slaves are usually very small, time delay between slaves is omitted in this paper. In contrast, the distance between master and slaves is large, and thus time delay is considered in (4).

Several notations are defined in *Appendix A*. With these notations, the following theorem is given.

Theorem 1: Consider TCPS (1) with controller (4) and Assumption 1. If there exist positive definite matrices W_r, R_{mr}, R_{sr}, S_r, R_r, P_1, P_2 and matrices X_r, N_r, M_r, $H_{\alpha m}$, H_{km}, $H_{\alpha r}$, H_{kr}, $\forall r = 1, \cdots, N$ with proportional dimensions such that the following matrix inequalities hold

$$\Phi < 0 \qquad (6)$$

$$\Phi_{1r} = \begin{bmatrix} \tilde{R}_r & X_r \\ * & \tilde{R}_r \end{bmatrix} > 0 \qquad (7)$$

and $\varepsilon\,(Q, \rho) \subset \{L(H_{\alpha m}, 0, H_{km}, H_{km}) \cap [\cap_{r=1}^{N} L(0, H_{\alpha r}, H_{kr}, H_{kr})]\}$ where $L(H_{\alpha m}, 0, H_{km}, H_{km}) = \{\dot{q}_m, \dot{q}_r, q_m, q_r \in \mathcal{R}^n : \left|\frac{1}{N}\sum_{r=1}^{N}(h_{kmi}q_m - h_{kmi}q_r + h_{\alpha mi}\dot{q}_m)\right| \le M_{\max,i},\ i = 1, \cdots, n\}$ and $L(0, H_{\alpha r}, H_{kr}, H_{kr}) = \{\dot{q}_m, \dot{q}_r, q_m, q_r \in \mathcal{R}^n : |h_{kri}q_m - h_{kri}q_r + h_{\alpha ri}\dot{q}_r| \le M_{\max,i},\ i = 1, \cdots, n\}$, h_{kmi} is the ith row of H_{km}, the same with $h_{\alpha mi}$, h_{kri} and $h_{\alpha ri}$, then closed-loop TCPS (1) is stable. Moreover, the estimate of DOA for (1) is $\Gamma = \{\dot{q}_{m0}, \dot{q}_{sr0}, q_{m0} - q_{sr0} : \Gamma_\delta \le 1\}$.

Proof: Choose Lyapunov function $V = \sum_{i=1}^{5} V_i$ with

$$\begin{aligned}
V_1 &= \dot{q}_m^T M_m(q_m)\dot{q}_m + \sum_{r=1}^{N} \dot{q}_r^T M_r(q_r)\dot{q}_r\\
&\quad + 2\int_0^t (\dot{q}_m^T(\sigma) F_h(\sigma) - \sum_{r=1}^{N} \dot{q}_r^T(\sigma) F_r(\sigma))d\sigma,\\
V_2 &= \sum_{r=1}^{N} e_r^T W_r e_r,\\
V_3 &= \sum_{r=1}^{N} \int_{t-\hat{d}_r}^{t-d_r(t)} e_r^T(\sigma) S_r e_r(\sigma)\, d\sigma,\\
V_4 &= \sum_{r=1}^{N} \int_{-\hat{d}_{ms}}^{0}\int_{t+\theta}^{t} \dot{q}_m^T(\sigma) R_{mr}\dot{q}_m(\sigma)\, d\sigma d\theta\\
&\quad + \sum_{r=1}^{N} \int_{-\hat{d}_{sm}}^{0}\int_{t+\theta}^{t} \dot{q}_r^T(\sigma) R_{sr}\dot{q}_r(\sigma)\, d\sigma d\theta\\
&\quad + \sum_{r=1}^{N} \int_{-\hat{d}_r}^{0}\int_{t+\theta}^{t} \dot{e}_r^T(\sigma) R_r\dot{e}_r(\sigma)\, d\sigma d\theta,\\
V_5 &= \theta_1^T P_1\theta_1 + \theta_2^T P_2\theta_2,
\end{aligned}$$

where $\theta_1^T = [\int_{t-d_1(t)}^{t} e_1^T(\sigma)d\sigma, \cdots, \int_{t-d_N(t)}^{t} e_N^T(\sigma)d\ \sigma]$, $\theta_2^T = [\int_{t-\hat{d}_1}^{t-d_1(t)} e_1^T(\sigma)d\sigma, \cdots, \int_{t-\hat{d}_N}^{t-d_N(t)} e_N^T(\sigma)d\ \sigma]$ and $e_r = q_m - q_r$.

Obviously, it is obtained that $V > 0$.

Based on Property 2 and Assumption 2, $\dot{V}_1$ is given as

$$\begin{aligned}
\dot{V}_1 &= 2\dot{q}_m^T \mathrm{sat}\Big(\frac{1}{N}\sum_{i=1}^{N}(-K_m(q_m - q_i(t - d_{im})) - \alpha_m\dot{q}_m)\\
&\quad + 2\sum_{i=1}^{N} \dot{q}_i^T \mathrm{sat}(K_i(q_m(t - d_{mi}) - q_i) - \alpha_i\dot{q}_i). \qquad (8)
\end{aligned}$$

From Lemma 1, $\dot{V}_1$ can be expressed as

$$\begin{aligned}
\dot{V}_1 &= 2\dot{q}_m^T \sum_{i=1}^{2^n} \eta_i \sum_{r=1}^{N} \frac{1}{N}\{(D_i^- H_{km} - D_i K_m)(q_m - q_r\\
&\quad + \int_{t-d_{rm}(t)}^{t} \dot{q}_r(\sigma)\, d\sigma) + (-D_i\alpha_m + D_i^- H_{\alpha m})\dot{q}_m\}\\
&\quad + \sum_{i=1}^{2^n}\sum_{r=1}^{N} 2\dot{q}_r^T \eta_i\{(D_i K_r + D_i^- H_{kr})(q_m - q_r\\
&\quad - \int_{t-d_{mr}(t)}^{t} \dot{q}_m(\sigma)\, d\sigma) + (-D_i\alpha_r + D_i^- H_{\alpha r})\dot{q}_r\}. \qquad (9)
\end{aligned}$$

The time derivative of V_4 is given by

$$\dot{V}_4 = \sum_{r=1}^{N}[\hat{d}_{ms}\dot{q}_m^T R_{mr}\dot{q}_m - \int_{t-\hat{d}_{ms}}^{t}\dot{q}_m^T(\sigma)R_{mr}\dot{q}_m(\sigma)d\sigma + \hat{d}_{sm}\dot{q}_r^T R_{sr}\dot{q}_r - \int_{t-\hat{d}_{sm}}^{t}\dot{q}_r^T(\sigma)R_{sr}\dot{q}_r(\sigma)d\sigma + \hat{d}_r\dot{e}_r^T R_r\dot{e}_r - \int_{t-\hat{d}_r}^{t}\dot{e}_r^T(\sigma)R_r\dot{e}_r(\sigma)d\sigma]. \quad (10)$$

By applying Lemma 2 and $-\int_{t-\hat{d}_r}^{t}\dot{e}_r^T(\sigma)R_r\dot{e}_r(\sigma)d\sigma = -\int_{t-\hat{d}_r}^{t-d_r(t)}\dot{e}_r^T(\sigma)R_r\dot{e}_r(\sigma)d\sigma - \int_{t-d_r(t)}^{t}\dot{e}_r^T(\sigma)R_r\dot{e}_r(\sigma)d\sigma$, we have the following conclusion

$$-\int_{t-\hat{d}_r}^{t}\dot{e}_r^T(\sigma)R_r\dot{e}_r(\sigma)d\sigma \le \frac{-1}{d_r(t)}(\int_{t-d_r(t)}^{t}\dot{e}_r(\sigma)d\sigma)^T R_r(\int_{t-d_r(t)}^{t}\dot{e}_r(\sigma)d\sigma) - \frac{3}{d_r(t)}\epsilon_2^T R_r\epsilon_2$$

where $\epsilon_2 = e_r(t) + e_r(t-d_r(t)) - \frac{2}{d_r(t)}\int_{t-d_r(t)}^{t}e_r(\sigma)d\sigma$.

We apply the Jensen inequality, then we can have

$$-\int_{t-d_{mr}(t)}^{t}\dot{q}_m^T(\sigma)R_{mr}\dot{q}_m(\sigma)d\sigma \le \frac{-1}{\hat{d}_{ms}}(\int_{t-d_{mr}(t)}^{t}\dot{q}_m(\sigma)d\sigma)^T R_{mr}(\int_{t-d_{mr}(t)}^{t}\dot{q}_m(\sigma)d\sigma).$$

Similar results are obtained by $\int_{t-\hat{d}_{sm}}^{t}\dot{q}_r^T(\sigma)R_{sr}\dot{q}_r(\sigma)d\sigma$. If there exists a matrix X_r such that $\Phi_{1r} > 0$, one has

$$-\int_{t-\hat{d}_r}^{t}\dot{e}_r^T(\sigma)R_r\dot{e}_r d\sigma \le -\frac{1}{\hat{d}_r}\xi^T\Gamma_r^T\Phi_{1r}\Gamma_r\xi \quad (11)$$

with $\xi^T = [\xi_1, \cdots, \xi_{10}]$ where $\xi_1 = [\dot{q}_m^T, \dot{q}_1^T, \cdots, \dot{q}_N^T]$, $\xi_2 = [\int_{t-d_{m1}(t)}^{t}\dot{q}_m^T(\sigma)d\sigma, \cdots, \int_{t-d_{mN}(t)}^{t}\dot{q}_m^T(\sigma)d\sigma]$, $\xi_3 = [\int_{t-d_{1m}(t)}^{t}\dot{q}_1^T(\sigma)d\sigma, \cdots, \int_{t-d_{Nm}(t)}^{t}\dot{q}_N^T(\sigma)d\sigma]$, $\xi_4 = [e_1^T, \cdots, e_N^T]$, $\xi_5 = [e_1^T(t-d_1(t)), \cdots, e_N^T(t-d_N(t))]$, $\xi_6 = [e_1^T(t-\hat{d}_1), \cdots, e_N^T(t-\hat{d}_N)]$, $\xi_7 = [\frac{1}{d_1(t)}\int_{t-d_1(t)}^{t}e_1^T(\sigma)d\sigma, \cdots, \frac{1}{d_N(t)}\int_{t-d_N(t)}^{t}e_N^T(\sigma)d\sigma]$, $\xi_8 = [\frac{1}{\hat{d}_1-d_1(t)}\int_{t-\hat{d}_1}^{t-d_1(t)}e_1^T(\sigma)\times d\sigma, \cdots, \frac{1}{\hat{d}_N-d_N(t)}\int_{t-\hat{d}_N}^{t-d_N(t)}e_N^T(\sigma)d\sigma]$, $\xi_9 = [\int_{t-d_1(t)}^{t}\dot{e}_1^T(\sigma)\times d\sigma, \cdots, \int_{t-d_N(t)}^{t}\dot{e}_N^T(\sigma)d\sigma]$, and $\xi_{10} = [\int_{t-\hat{d}_1}^{t-d_1(t)}\dot{e}_1^T(\sigma)d\sigma, \cdots, \int_{t-\hat{d}_N}^{t-d_N(t)}\dot{e}_N^T(\sigma)d\sigma]$.

With the above results, one has

$$\dot{V}_4 \le \sum_{r=1}^{N}[\hat{d}_{ms}\dot{q}_m^T R_{mr}\dot{q}_m - \frac{1}{\hat{d}_{ms}}(\int_{t-d_{mr}(t)}^{t}\dot{q}_m(\sigma)d\sigma)^T \times R_{mr}(\int_{t-d_{mr}(t)}^{t}\dot{q}_m(\sigma)d\sigma) + \hat{d}_{sm}\dot{q}_r^T R_{sr}\dot{q}_r - \frac{1}{\hat{d}_{sm}} \times (\int_{t-d_{rm}(t)}^{t}\dot{q}_r(\sigma)d\sigma)^T R_{rm}(\int_{t-d_{rm}(t)}^{t}\dot{q}_r(\sigma)d\sigma) + \hat{d}_r\dot{e}_r^T R_r\dot{e}_r - \frac{1}{\hat{d}_r}\xi^T\Gamma_r^T\Phi_{1r}\Gamma_r\xi]. \quad (12)$$

Calculation of $\dot{V}_2$, $\dot{V}_3$ and $\dot{V}_5$ is omitted due to the limited space. For $r = 1, \cdots, N$, the following free-weighting matrices are considered, i.e., $n_r = 2\xi^T N_r[e_r(t) - e_r(t-d_r(t)) - \int_{t-d_r(t)}^{t}\dot{e}_r(\sigma)d\sigma] = 0$ and $m_r = 2\xi^T M_r[e_r(t-d_r(t)) - e_r(t-\hat{d}_i) - \int_{t-\hat{d}_i}^{t-d_r(t)}\dot{e}_r(\sigma)d\sigma] = 0$. Therefore, we have

$$\dot{V} = \sum_{i=1}^{5}\dot{V}_i + \sum_{r=1}^{N}(n_r + m_r) \le \sum_{i=1}^{2^n}\eta_i\xi^T\Phi\xi. \quad (13)$$

Under (6) and (7), we have $\dot{V} < 0$ for $\forall x \in \varepsilon(Q,\rho)\backslash\{0\} \in L(H_{\alpha m}, 0, H_{km}, H_{km}) \cap [\cap_{r=1}^{N}L(0, H_{\alpha r}, H_{kr}, H_{kr})]$. Then, $x^T Q x \le V(x_0) \le (\hat{\varrho}_m + \sum_{r=1}^{N}\frac{1}{2}\hat{d}_{ms}^2\lambda_{\max}(R_{mr}))\delta_{m1}^2 + \sum_{r=1}^{N}\hat{\varrho}_r\delta_{sr1}^2 + \sum_{r=1}^{N}\frac{1}{2}\hat{d}_{sm}^2\lambda_{\max}(R_{sr})\delta_{sr1}^2 + \sum_{r=1}^{N}(\lambda_{\max}(W_r) + (\hat{d}_r - \check{d}_r)\lambda_{\max}(S_r) + \hat{d}_r^2\lambda_{\max}(P_1) + (\hat{d}_r - \check{d}_r)^2\lambda_{\max}(P_2))\delta_{er1}^2 + \sum_{r=1}^{N}\frac{1}{2}\hat{d}_r^2\lambda_{\max}(R_r)\delta_{er2}^2 = \Gamma_\delta$. The estimation of DOA is obtained from $\Gamma_\delta \le 1$. ■

Remark 2: In Theorem 1, $\dot{V} < 0$ with $\Phi < 0$ and $\Phi_{1r} > 0$ for all $(d_i(t), \dot{d}_i(t)) \in [\check{d}_i, \hat{d}_i] \times [\check{\mu}_i, \hat{\mu}_i]$. As Φ is a convex matrix with respect to $d_i(t)$ and $\dot{d}_i(t)$, it is required to guarantee $\Phi < 0$ at the vertices of the interval $[\check{d}_i, \hat{d}_i] \times [\check{\mu}_i, \hat{\mu}_i]$. Thus, $\Phi < 0$ can be solved as LMIs optimization problem. With the LMIs Toolbox in MATLAB, the above inequalities are feasible and easily computed.

It is interesting to come up with a solution such that the estimate of DOA is maximized. In our previous work [16], we have provided an LMI-based strategy to choose the desired parameters for the single-slave TCPS. The proposed strategy in [16] can provide a guideline to choose the desired parameters, and then the following optimization problem is obtained.

$$\begin{aligned}
&\min\ \varpi\\
&s.t.\ a)\ \omega_i > 0, \quad i = 1, 2, \ldots, 7,\\
&\quad W_r > 0, \quad S_r > 0,\ R_{mr} > 0,\ R_{sr} > 0,\\
&\quad R_r > 0, \quad P_1 > 0,\ P_2 > 0,\ r = 1, 2, \ldots, N\\
&\quad b)\ \omega_r I - W_r \ge 0, \quad \alpha_r I - S_r \ge 0,\\
&\quad \beta_r I - R_{mr} \ge 0, \quad \varrho_r I - R_{sr} \ge 0,\\
&\quad \varkappa_r I - R_r \ge 0, \quad \upsilon_1 I - P_1 \ge 0,\\
&\quad \upsilon_2 I - P_2 \ge 0\\
&\quad c)\ \varepsilon(Q,1) \subset \{L(H_{\alpha m}, 0, H_{km}, H_{km})\\
&\quad \cap [\cap_{r=1}^{N}L(0, H_{\alpha r}, H_{kr}, H_{kr})]\}\\
&\quad d)\ \text{LMIs (6) and (7)},
\end{aligned}$$

where $\varpi = \sum_{r=1}^{N}\omega_r + (\hat{d}_r - \check{d}_r)\alpha_r + \frac{1}{2}\hat{d}_{ms}^2\beta_r + \frac{1}{2}\hat{d}_{sm}^2\varrho_r + \frac{1}{2}\hat{d}_r^2\varkappa_r + \hat{d}_r^2\upsilon_1 + (\hat{d}_r - \check{d}_r)^2\upsilon_2$.

The constraint b) is equivalent to $\lambda_{\max}(W_r) \le \omega_r$. The same holds for others. With Property 1, we get $\sum_{r=1}^{N}\lambda_{\max}(W_r) + (\hat{d}_r - \check{d}_r)\lambda_{\max}(S_r) + \frac{1}{2}\hat{d}_{ms}^2\lambda_{\max}(R_{mr}) + \frac{1}{2}\hat{d}_{sm}^2\lambda_{\max}(R_{sr}) + \frac{1}{2}\hat{d}_r^2\lambda_{\max}(R_r) + \hat{d}_r^2\lambda_{\max}(P_1) + (\hat{d}_r - \check{d}_r)^2\lambda_{\max}(P_2) \le \varpi$. Then a maximized estimate of DOA is obtained by $\delta_{\max} = \frac{1}{\sqrt{\varpi}}$. Furthermore, if the lower bound of delay is fixed, the estimate of DOA varies inversely with the size of time delay, i.e., the larger the range of delay is,

the smaller the estimate of DOA is. For simplicity, the optimization is considered for the case $\delta_{m1} = \delta_{sr1} = \delta_{er1} = \delta_{er2}$. We can fix some parameters and optimize others by the same way.

B. DESIGN OF DECENTRALIZED CONSENSUS CONTROLLER

In Section III-A, the consensus controller (4) is based on a centralized mode, where master is required to acquire all slaves' state information and there is no cooperation among slaves. However, the applications of centralized implementation are not feasible in large-scale networks. To overcome this shortage, this section designs a decentralized consensus controller, where each slave cooperates with its neighbors to accomplish the cooperative consensus.

The prerequisite of cooperation is connectivity maintenance through the installed sensors. As mentioned in Section II-B, sensing sensor for each slave robot i $(i = 1, \cdots, N)$ is mounted at the base of each manipulator, and the position of this sensor is denoted by $p_i \in \mathcal{R}^3$. Combining with connectivity maintenance, this section uses min-weighted rigid graph to optimize the neighborhood relationship of slave robots. With the optimized communication topology, a decentralized consensus controller is designed to compensate the time-varying delay and saturation effects. As it is mentioned above, the min-weighted rigid graph is infinitesimally rigid. Then, referring to the properties of infinitesimally rigidity, we know that the topology in min-weighted rigid graph is connected. Thus, the min-weighted rigid graph can guarantee the connectivity maintenance.

In the following, we attempt to design a topology optimization scheme. By analyzing the relationship between local rigidity and global rigidity of a graph, we give the following properties.

- If an arbitrary vertex $i \in \mathcal{V}$ and its neighbors $\mathcal{N}_i(|\mathcal{N}_i|_\# \geq d)$ compose the min-weighted rigid subgraph $\acute{\mathcal{G}} = (\acute{\mathcal{V}}, \acute{\mathcal{E}})$, then it is concluded that $\mathcal{G} = (\mathcal{V}, \mathcal{E})$ is rigid, where $\acute{\mathcal{V}} = \{i, \mathcal{N}_i\}$ and $\acute{\mathcal{E}} \subseteq \mathcal{E}$.
- If any framework $\acute{\mathcal{G}} = (\acute{\mathcal{V}}, \acute{\mathcal{E}})$ of a rigid graph $\mathcal{G} = (\mathcal{V}, \mathcal{E})$ is replaced with any other rigid graph $\tilde{\mathcal{G}} = (\tilde{\mathcal{V}}, \tilde{\mathcal{E}})$, it is concluded that the obtained global graph is still rigid.

With above properties, we have the following lemma.

Lemma 3: [19] For vertex $i \in \mathcal{V}$, $\mathcal{G}_i = (\breve{\mathcal{V}}_i, \breve{\mathcal{E}}_i)$ is denoted as local min-weighted rigid graph which consists of vertex i and $\mathcal{N}_i(|\mathcal{N}_i|_\# \geq d)$, and $\mathcal{G} = (\mathcal{V}, \mathcal{E}) = \cup_{i\in\mathcal{V}}\mathcal{G}_i$. Define another edge set $\vec{\mathcal{E}} = \{e = (k, l) \in \mathcal{E} : k, l \in \breve{\mathcal{V}}_i$, and $e \notin \breve{\mathcal{E}}_i\}$. Then, $\mathcal{G}^m = (\mathcal{V}, \mathcal{E}/\vec{\mathcal{E}})$ is the global min-weighted rigid graph.

With Lemma 3, Algorithm 1 is provided to obtain the min-weighted rigid graph for slave robots. Compared with "neighborhood rule" based topology, the communication links of slave robots in min-weighted rigid graph are minimum on the condition of rigidity retaining. Additionally, the sum of the energy balance weights for sensor nodes is also the minimum. Algorithm 1 is summarized as: 1) Obtain the local min-weighted rigid graph for slave robots; 2) Delete the edges which are not in the global min-weighted rigid graph.

Algorithm 1 Design of Topology Optimization Scheme

Input: A local unoptimized graph $\mathcal{G}_i^o = (\mathcal{V}_i, \mathcal{E}_i^o)$, and $\mathcal{E}_i^o$ is defined as follows: if $\|p_i - p_j\| < r$, $(i, j) \in \mathcal{E}_i^o$; otherwise, $(i, j) \notin \mathcal{E}_i^o$

Output: The global min-weighted rigid graph

```
for i = 1 : N do
    Sequence the edges in E_i^o based on the length sizes from small beginnings, and then build the rigidity matrix R(G_i^o)
    Initialize R(G_i^m) as the first row of R(G_i^o)
    for j = 1 : |E_i^o|_# do
        while rank(R(G_i^m)) ≤ 3N − 6 do
            Add the next row of R(G_i^o) to R(G_i^m) to form a new matrix R⃗(G_i^m)
            if R⃗ is full rank then
                R(G_i^m) = R⃗(G_i^m) and record E_i^m in R⃗(G_i^m) corresponding to the row
    Delete the edges satisfying the conditions in Lemma 3
return G^m = (V, E^m)
```

Under the optimized communication topology, the decentralized consensus controller is designed as

$$\begin{aligned}\tau_m &= \text{sat}(\sum_{i=1}^{N} b_i K_m(q_i(t - d_{im}) - q_m) - \alpha_m \dot{q}_m) + G_m(q_m)\\ \tau_i &= \text{sat}(\sum_{j=1}^{N} a_{ij} K_i(q_i - q_j) + b_i K_i(q_m(t - d_{mi})\\ &\quad - \bar{q}_i) - \alpha_i \dot{q}_i) + G_i(\bar{q}_i),\end{aligned} \tag{14}$$

where $\forall i = 1, \cdots, N$. $K_m \in \mathcal{R}^{n\times n}$, $\alpha_m \in \mathcal{R}^{n\times n}$, $K_i \in \mathcal{R}^{n\times n}$ and $\alpha_i \in \mathcal{R}^{n\times n}$ are gain matrices to be designed. $b_i > 0$ if master can exchange information with slave i, and $b_i = 0$ otherwise. With Property 3, one obtains that $|G_{ir}(q)| < \vartheta_r$ for $\forall r = 1, \ldots, n$. As such, the rth element $M_{\max,r}$ of $M_{\max}$ satisfies $M_{\max,r} \leq T_r - \vartheta_r$. The control framework is shown in Fig. 4.

The property of connectivity maintenance in Algorithm 1 is given by the following theorem.

Theorem 2: After the neighborhood topology relationship of slave robots is schematically denoted by a min-weighted rigid graph $\mathcal{G}^m$ with Algorithm 1, we have the following conclusions: 1) The topology $\mathcal{G}^m$ is 3-connected; 2)The average degree of each slave robot is 6.

Proof: With Algorithm 1, min-weighted rigid graph $\mathcal{G}^m$ is generated. As mentioned above, a graph is rigid if the only smooth motions are those corresponding to translation and rotation of the whole formation (see [29], [30] for a precise definition), thus each slave in rigid graph has at least three neighbors for rigidity requirement. This means any two slaves have at least three connected paths, i.e., the topology $\mathcal{G}^m$ is 3-connected.

There are $3N - 6$ communication links for N slave robots. It is noticed that the sum of the degree for all slaves is

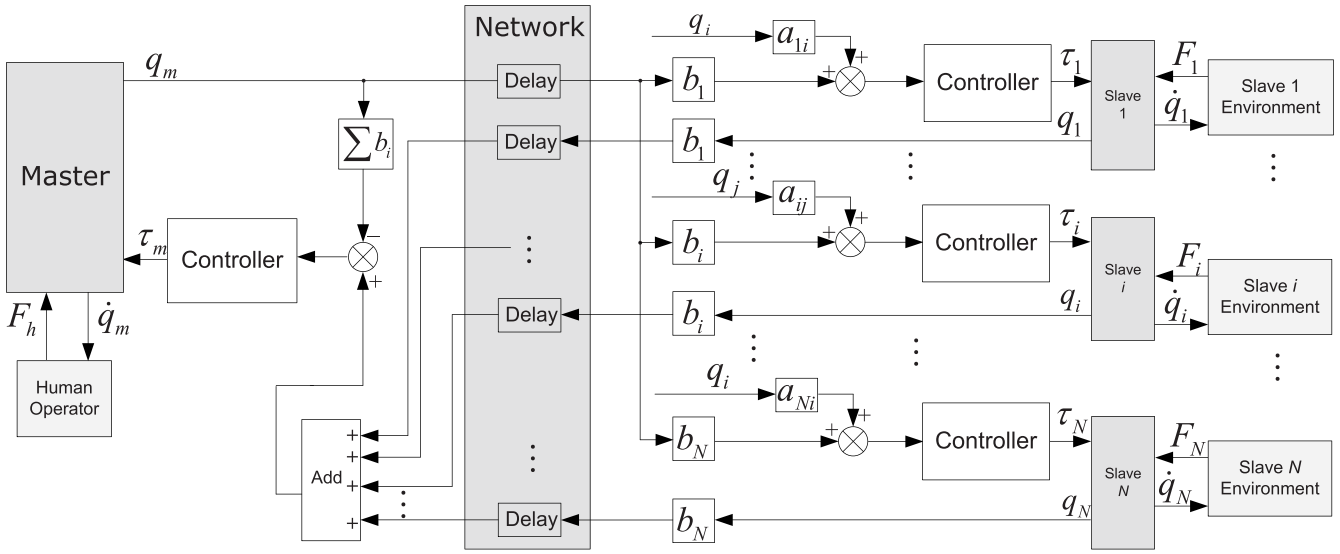

FIGURE 4. Control framework of the decentralized consensus controller.

the twice of the number of communication links. Denote the average degree of each slave robot as $\bar{D}$, thus we have $\bar{D} = 2(3N-6)/N$. Therefore, $\lim_{N\to\infty}\bar{D} = 6$. ■

The bounds of the initial values are defined as (5), $\max_{\theta\in[-d_2,0]} \|q_{i0}(\theta) - q_{j0}(\theta)\| \le \delta_{eij3}$, and $\max_{\theta\in[-d_2,0]} \|\dot{q}_{i0}(\theta) - \dot{q}_{j0}(\theta)\| \le \delta_{eij4}$, where δ_{m1}, δ_{sr1}, δ_{er1}, δ_{er2}, δ_{eij3}, δ_{eij4} are positive parameters. The stability conditions for (14) is given in Theorem 3. Several notations are defined in *Appendix B*.

Theorem 3: Consider the TCPS (1) with decentralized controller (14) and optimized topology. The TCPS (1) is stable, if there exist positive definite matrices R_{mr}, R_{sr}, S_r, W_r, Z_r, U_r, Q_r, R_r, P_{1r}, P_{2r}, P_{3r}, P_{4r} and matrices X_r, Y_r, N, M, G, H, $H_{\alpha m}$, H_{km}, $H_{k\alpha r}$, H_{kbr}, $H_{\alpha r}$ $\forall r = 1,\cdots,N$ with proportional dimensions such that the following matrix inequalities hold

$$\hat{\Phi} < 0, \quad \breve{R}_i > 0, \quad \breve{Q}_i > 0 \tag{15}$$

and $\varepsilon\ (\Omega,\rho)\subset\{L(H_{\alpha m},H_{km})\cap[\cap_{r=1}^{N}L(H_{k\alpha r},H_{kbr},H_{\alpha r})]\}$, where $L(H_{\alpha m},H_{km}) = \{\dot{q}_m,\dot{q}_r,q_m,q_r \in \mathcal{R}^n : \left|\sum_{r=1}^{N} b_r(h_{kmi}q_m - h_{kmi}q_r) + h_{\alpha mi}\dot{q}_m)\right| \le M_{\max,i},\ i = 1,\cdots,n\}$, $L(H_{k\alpha r},H_{kbr},H_{\alpha r}) = \{\dot{q}_m,\dot{q}_r,q_m,q_r \in \mathcal{R}^n : \left|\sum_{r=1}^{N}\sum_{p=1}^{N} a_{rp}(h_{kari}q_r - h_{kari}q_p) + \sum_{r=1}^{N} b_r(h_{kbri}q_m - h_{kbri}q_r) + h_{\alpha ri}\dot{q}_r\right| \le M_{\max,i},\ i = 1,\cdots,n\}$, h_{kmi}, $h_{\alpha mi}$, h_{kari}, h_{kbri} and $h_{\alpha ri}$ are the ith row of H_{km}, H_{km}, $H_{k\alpha r}$, H_{kbr} and $H_{\alpha r}$ respectively. The estimate of DOA for (14) is $\Gamma = \{\dot{q}_{m0},\dot{q}_{sr0},q_{m0},q_{sr0} : \hat{\Gamma}_\delta \le 1\}$.

Proof: Choose Lyapunov function $V = \sum_{i=1}^{5} V_i$ with

$$V_1 = \dot{q}_m^T M_m(q_m)\dot{q}_m + \sum_{i=1}^{N}\dot{q}_i^T M_i(q_i)\dot{q}_i + 2\int_0^t (\dot{q}_m^T(\sigma)F_h(\sigma) - \sum_{i=1}^{N}\dot{q}_i^T(\sigma)F_r(\sigma))d\sigma,$$

$$V_2 = \sum_{i=1}^{N}\left\{b_i e_{mi}^T W_i e_{mi} + \sum_{j=1}^{N} a_{ij} e_{ij}^T Z_i e_{ij}\right\},$$

$$V_3 = \sum_{i=1}^{N}\left\{b_i\int_{t-\hat{d}_i}^{t-d_i(t)} e_{mi}^T(\sigma)S_i e_{mi}(\sigma)\,d\sigma + \sum_{j=1}^{N} a_{ij}\int_{t-\hat{d}_i}^{t-d_i(t)} e_{ij}^T(\sigma)U_i e_{ij}(\sigma)\,d\sigma\right\},$$

$$V_4 = \sum_{i=1}^{N}\left\{b_i\int_{-\hat{d}_{ms}}^{0}\int_{t+\theta}^{t}\dot{q}_m^T(\sigma)R_{mi}\dot{q}_m(\sigma)\,d\sigma d\theta + b_i\int_{-\hat{d}_{sm}}^{0}\int_{t+\theta}^{t}\dot{q}_i^T(\sigma)R_{si}\dot{q}_i(\sigma)\,d\sigma d\theta + b_i\int_{-\hat{d}_i}^{0}\int_{t+\theta}^{t}\dot{e}_{mi}^T(\sigma)R_i\dot{e}_{mi}(\sigma)\,d\sigma d\theta + \sum_{j=1}^{N} a_{ij}\int_{-\hat{d}_i}^{0}\int_{t+\theta}^{t}\dot{e}_{ij}^T(\sigma)Q_i\dot{e}_{ij}(\sigma)\,d\sigma d\theta\right\},$$

$$V_5 = \sum_{i=1}^{N}\left\{b_i(\int_{t-d_i(t)}^{t} e_{mi}(\sigma)\,d\sigma)^T P_{1i}(\int_{t-d_i(t)}^{t} e_{mi}(\sigma) \times d\sigma) + b_i(\int_{t-\hat{d}_i}^{t-d_i(t)} e_{mi}(\sigma)\,d\sigma)^T P_{2i}(\int_{t-\hat{d}_i}^{t-d_i(t)} e_{mi}(\sigma) \times d\sigma) + \sum_{j=1}^{N} a_{ij}(\int_{t-d_i(t)}^{t} e_{ij}(\sigma)\,d\sigma)^T P_{3i} \times (\int_{t-d_i(t)}^{t} e_{ij}(\sigma)\,d\sigma) + \sum_{j=1}^{N} a_{ij}(\int_{t-\hat{d}_i}^{t-d_i(t)} e_{ij}(\sigma) \times d\sigma)^T P_{4i}(\int_{t-\hat{d}_i}^{t-d_i(t)} e_{ij}(\sigma)\,d\sigma)\right\}, \tag{16}$$

where $e_{mi} = q_m - q_i$ and $e_{ij} = q_i - q_j$.

Clearly, $V > 0$. With Property 2 and Assumption 2, $\dot{V}_1$, $\dot{V}_2$, and $\dot{V}_3$ are given as

$$\dot{V}_1 = 2\dot{q}_m^T[\sum_{i=1}^{N} b_i(-D_rK_m + D_r^-H_{km})(q_i(t-d_{im}(t)) - q_m) + (-D_r\alpha_m + D_r^-H_{\alpha m})\dot{q}_m] + 2\sum_{i=1}^{N}\dot{q}_i^T \times [\sum_{j=1}^{N} a_{ij}(D_rK_i + D_r^-H_{kai})(q_i - q_j) + b_i(D_rK_i + D_r^-H_{kbi})(q_m(t-d_{mi}(t)) - q_i) \times (-D_r\alpha_i + D_r^-H_{\alpha i})q_i].$$

$$\begin{aligned}\dot{V}_2 &= 2\sum_{i=1}^{N} b_i[\dot{q}_m^T W_i e_{mi} - \dot{q}_i^T W_i e_{mi}] \\ &\quad + 2\sum_{i=1}^{N}\sum_{j=1}^{N} a_{ij}[\dot{q}_i^T Z_i e_{ij} - \dot{q}_i^T Z_i e_{ij}], \\ \dot{V}_3 &= \sum_{i=1}^{N} b_i[(1-\dot{d}_i(t))e_{mi}^T(t-d_i(t))W_i e_{mi}(t-d_i(t)) \\ &\quad - e_{mi}^T(t-\hat{d}_i)W_i e_{mi}(t-\hat{d}_i) + \sum_{i=1}^{N}\sum_{j=1}^{N} a_{ij} \\ &\quad \times [(1-\dot{d}_i(t))e_{ij}^T(t-d_i(t))U_i e_{mi}(t-d_i(t)) \\ &\quad - e_{ij}^T(t-\hat{d}_i)U_i e_{ij}(t-\hat{d}_i)]. \end{aligned} \tag{17}$$

With Lemma 1 and $\varepsilon\ (\Omega,\rho) \subset \{L(H_{\alpha m}, H_{km}) \cap [\cap_{r=1}^{N} L(H_{k\alpha r}, H_{kbr}, H_{\alpha r})]\}$, $\dot{V}_1$ can be further expressed as

$$\begin{aligned}\dot{V}_1 &= \sum_{r=1}^{2^n} \eta_r\{2\dot{q}_m^T[\sum_{i=1}^{N} b_i(-D_r K_m + D_r^- H_{km})(e_{mi} \\ &\quad + \int_{t-d_{im}(t)}^{t} \dot{q}_i(\sigma)d\sigma) + (-D_r\alpha_m + D_r^- H_{\alpha m})\dot{q}_m] \\ &\quad + 2\sum_{i=1}^{N} \dot{q}_i^T[\sum_{j=1}^{N} a_{ij}(D_r K_i + D_r^- H_{kai})e_{ij} \\ &\quad + b_i(D_r K_i + D_r^- H_{kbi})(e_{mi} - \int_{t-d_{mi}(t)}^{t} \dot{q}_m(\sigma)d\sigma) \\ &\quad + (-D_r\alpha_i + D_r^- H_{\alpha i})\bar{q}_i]\}, \end{aligned} \tag{18}$$

where $0 < \eta_r \le 1$ and $\sum_{r=1}^{2^n} \eta_r = 1$.

The time derivative of V_4 is

$$\begin{aligned}\dot{V}_4 &= \sum_{i=1}^{N} \Big\{ b_i[\hat{d}_{ms}\dot{q}_m^T R_{mi}\dot{q}_m - \int_{t-\hat{d}_{ms}}^{t} \dot{q}_m^T(\sigma)R_{mi} \\ &\quad \times \dot{q}_m(\sigma)d\sigma + \hat{d}_{sm}\dot{q}_i^T R_{si}\dot{q}_i - \int_{t-\hat{d}_{sm}}^{t} \dot{q}_i^T(\sigma) \\ &\quad \times R_{si}\dot{q}_i(\sigma)d\sigma + \hat{d}_i\dot{e}_{mi}^T R_i\dot{e}_{mi} - \int_{t-\hat{d}_i}^{t} \dot{e}_{mi}^T(\sigma) \\ &\quad \times R_i\dot{e}_{mi}(\sigma)d\sigma] + \sum_{j=1}^{N} a_{ij}[\hat{d}_i\dot{e}_{ij}^T Q_i\dot{e}_{ij} \\ &\quad - \int_{t-\hat{d}_i}^{t} \dot{e}_{ij}^T(\sigma)Q_i\dot{e}_{ij}(\sigma)d\sigma] \Big\}. \end{aligned} \tag{19}$$

Based on Newton-Leibniz formula, the following equalities hold

$$\begin{aligned} n_i &= 2\xi^T N_i[e_{mi}(t) - e_{mi}(t-d_i(t)) - \int_{t-d_i(t)}^{t} \dot{e}_{mi}(\sigma)d\sigma] \\ &= 0, \\ m_i &= 2\xi^T M_i[e_{mi}(t-d_i(t)) - e_{mi}(t-\hat{d}_i) \\ &\quad - \int_{t-\hat{d}_i}^{t-d_i(t)} \dot{e}_{mi}(\sigma)d\sigma] \\ &= 0, \\ g_i &= 2\xi^T G_i[e_{ij}(t) - e_{ij}(t-d_i(t)) - \int_{t-d_i(t)}^{t} \dot{e}_{ij}(\sigma)d\sigma] \\ &= 0, \\ h_i &= 2\xi^T M_i[e_{mi}(t-d_i(t)) - e_{mi}(t-\hat{d}_i) \\ &\quad - \int_{t-\hat{d}_i}^{t-d_i(t)} \dot{e}_{mi}(\sigma)d\sigma] \\ &= 0, \end{aligned} \tag{20}$$

with

$$\xi^T = [\dot{q}_m^T, \xi_1, \cdots, \xi_{17}] \tag{21}$$

where $\xi_1 = [\dot{q}_1^T, \cdots, \dot{q}_N^T]$, $\xi_2 = [\int_{t-d_{mi_\nu}(t)}^{t} \dot{q}_m^T(\sigma)\,d\sigma]_{n\times\bar{\Im}_m n}$, $\xi_3 = [\int_{t-d_{i_\nu m}(t)}^{t} \dot{q}_{i_\nu}^T(\sigma)\,d\sigma]_{n\times\bar{\Im}_m n}$, $\xi_4 = [e_{mi_\nu}^T]_{n\times\bar{\Im}_m n}$, $\xi_5 = [e_{mi_\nu}^T(t-d_{i_\nu}(t))]_{n\times\bar{\Im}_m n}$, $\xi_6 = [e_{mi_\nu}^T(t-\hat{d}_{i_\nu})]_{n\times\bar{\Im}_m n}$, $\xi_{10} = [\frac{1}{d_{i_\nu}(t)} \times \int_{t-d_{i_\nu}(t)}^{t} e_{mi_\nu}^T(\sigma)\,d\sigma]_{n\times\bar{\Im}_m n}$, $\xi_{11} = [\frac{1}{\hat{d}_{i_\nu}-d_{i_\nu}(t)} \times \int_{t-\hat{d}_{i_\nu}}^{t-d_{i_\nu}(t)} e_{mi_\nu}^T(\sigma)]_{n\times\bar{\Im}_m n}$, $\xi_{12} = [\int_{t-d_{i_\nu}(t)}^{t} \dot{e}_{mi_\nu}^T(\sigma) \times d\sigma]_{n\times\bar{\Im}_m n}$, $\xi_{13} = [\int_{t-\hat{d}_{i_\nu}}^{t-d_{i_\nu}(t)} \dot{e}_{mi_\nu}^T(\sigma)]_{n\times\bar{\Im}_m n}$, $i_\nu \in \{1,2,\ldots,N | i_\nu \in \Im_m\}$, $\nu = 1,2,\ldots,\bar{\Im}_m$, $i_{\nu+1} = \text{ceil}(i_\nu)$, and ceil$(\cdot)$ is the ceil function (the smallest integer greater than or equal to). $\xi_7 = [e_{\nu j_p^\nu}^T]_{n\times\sum_{i=1}^{N}\bar{\Im}_i n}$, $\xi_8 = [e_{\nu j_p^\nu}^T(t-d_\nu(t))]_{n\times\sum_{i=1}^{N}\bar{\Im}_i n}$, $\xi_9 = [e_{\nu j_p^\nu}^T(t-\hat{d}_\nu)]_{n\times\sum_{i=1}^{N}\bar{\Im}_i n}$, $\xi_{14} = [\frac{1}{d_\nu(t)}\int_{t-d_\nu(t)}^{t} e_{\nu j_p^\nu}^T(\sigma)\,d\sigma]_{n\times\sum_{i=1}^{N}\bar{\Im}_i n}$, $\xi_{15} = [\frac{1}{\hat{d}_\nu-d_\nu(t)}\int_{t-\hat{d}_\nu}^{t-d_\nu(t)} e_{\nu j_p^\nu}^T(\sigma)]_{n\times\sum_{i=1}^{N}\bar{\Im}_i n}$, $j_{p+1}^\nu = \text{ceil}(j_p^\nu)$, $\xi_{16} = [\int_{t-d_\nu(t)}^{t} \dot{e}_{\nu j_p^\nu}^T(\sigma)\,d\sigma]_{n\times\sum_{i=1}^{N}\bar{\Im}_i n}$, and $\xi_{17} = [\int_{t-\hat{d}_\nu}^{t-d_\nu(t)} \dot{e}_{\nu j_p^\nu}^T(\sigma)]_{n\times\sum_{i=1}^{N}\bar{\Im}_i n}$, $j_p^\nu \in \{1,2,\ldots,N | a_{\nu j_p^\nu} \ne 0\}$, $p = 1,2,\ldots,\bar{\Im}_\nu$, $\nu = 1,2,\ldots,N$.

From (18) to (21), we have $\dot{V} = \sum_{i=1}^{5}\dot{V}_i + \sum_{r=1}^{N}(n_r + m_r + g_r + h_r) \le \sum_{i=1}^{2^n} \eta_i \xi^T \hat{\Phi}\xi$ for $x \in L(H_{\alpha m}, H_{km}) \cap [\cap_{r=1}^{N} L(H_{k\alpha r}, H_{kbr}, H_{\alpha r})]$. If (15) is satisfied, we have $\dot{V} < 0$ for $\forall x \in \varepsilon\ (\Omega,\rho)\backslash\{0\} \in L(H_{\alpha m}, H_{km}) \cap [\cap_{r=1}^{N} L(H_{k\alpha r}, H_{kbr}, H_{\alpha r})]$. Then, $x^T\Omega x \le V(x_t) < V(x_0) \le \Gamma_\delta$.The estimate of DOA is obtained from $\Gamma_\delta \le 1$. ■

Similar to the optimization in Section III-A, the following optimization problem is obtained

$$\begin{aligned} &\min\ \varpi \\ &\text{s.t. } a)\ \omega_i^j > 0, \quad i \in \Im_m, \quad j = 1,2,\ldots,7 \\ &\qquad \alpha_r^{\bar{j}} > 0, \quad r = 1,2,\ldots,N,\ \bar{j} = 1,2,\ldots,5 \\ &\qquad W_i > 0, \quad S_i > 0,\ R_{mi} > 0,\ R_{si} > 0, \\ &\qquad R_i > 0, \quad P_{1i} > 0,\ P_{2i} > 0, \\ &\qquad Z_r > 0, \quad U_r > 0,\ Q_r > 0,\ P_{3r} > 0,\ P_{4r} > 0 \\ &\quad b)\ \omega_i^1 I - W_i \ge 0, \quad \omega_i^2 I - S_i \ge 0, \\ &\qquad \omega_i^3 I - R_{mi} \ge 0, \quad \omega_i^4 I - R_{si} \ge 0, \\ &\qquad \omega_i^5 I - R_i \ge 0, \quad \omega_i^6 I - P_{1i} \ge 0,\ \omega_i^7 I - P_{2i} \ge 0, \\ &\qquad \alpha_r^1 I - Z_r \ge 0, \quad \alpha_r^2 I - U_r \ge 0,\ \alpha_r^3 I - Q_r \ge 0, \\ &\qquad \alpha_r^4 I - P_{3r} \ge 0, \quad \alpha_r^5 I - P_{4r} \ge 0 \\ &\quad c)\ \varepsilon\ (\Omega,\rho) \subset \{L(H_{\alpha m}, H_{km}) \\ &\qquad \cap[\cap_{r=1}^{N} L(H_{k\alpha r}, H_{kbr}, H_{\alpha r})]\} \\ &\quad d)\ \text{LMI (15)}, \end{aligned}$$

where $\varpi = \sum_{i\in\Im_m}(\omega_i^1 + (\hat{d}_r - \check{d}_r)\omega_i^2 + \frac{1}{2}\hat{d}_{ms}^2\omega_i^3 + \frac{1}{2}\hat{d}_{sm}^2\omega_i^4 + \frac{1}{2}\hat{d}_i^2\omega_i^5 + \hat{d}_i^2\omega_i^6 + (\hat{d}_r - \check{d}_r)^2\omega_i^7) + \sum_{r=1}^{N}(\alpha_r^1 + (\hat{d}_r - \check{d}_r)\alpha_r^2 + \frac{1}{2}\hat{d}_r^2\alpha_r^3 + +\hat{d}_i^2\alpha_r^4 + (\hat{d}_r - \check{d}_r)^2\alpha_r^5)$.

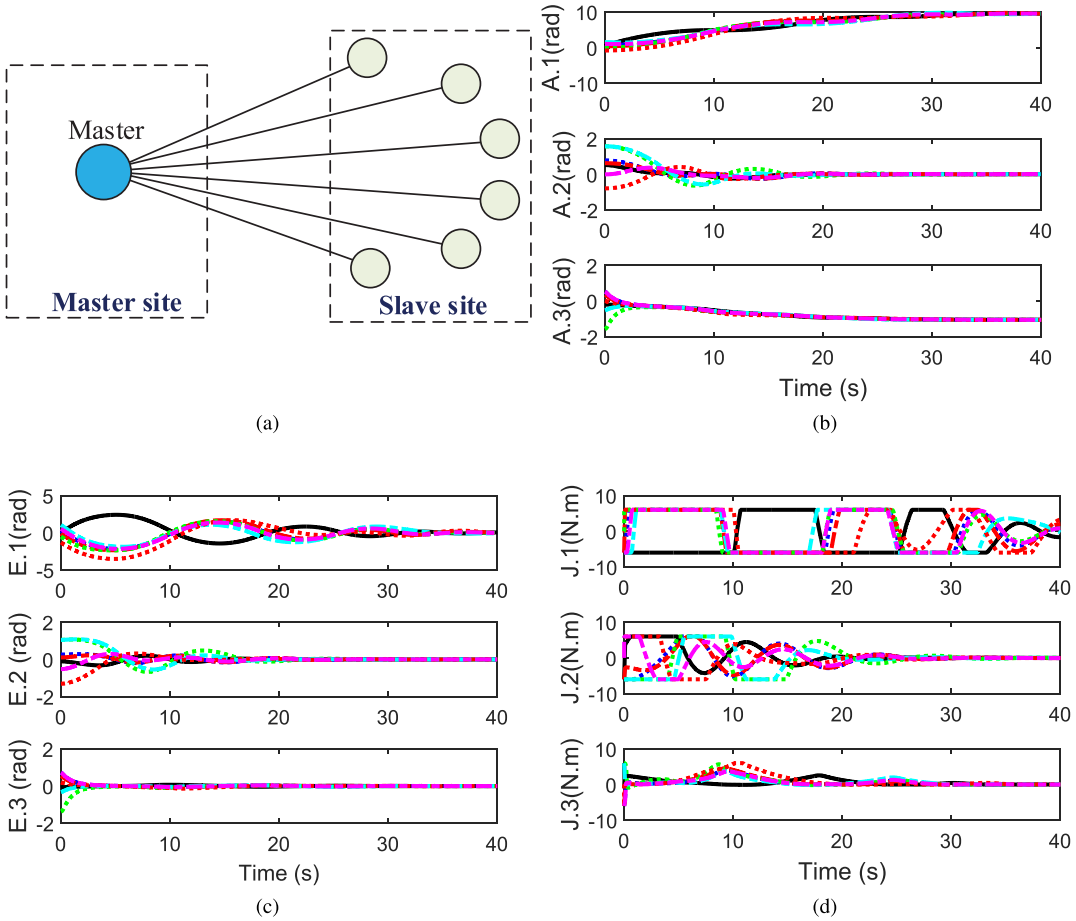

FIGURE 5. Simulation results for the centralized consensus controller (4). (a) Communication topology of master and slaves. (b) Angles of manipulators. (c) Consensus errors of angles. (d) Control torque for manipulators.

Similarly, $\sum_{i\in\Im_m}(\lambda_{\max}(W_i) + (\hat{d}_r - \check{d}_r)\lambda_{\max}(S_i) + \frac{1}{2}\hat{d}_{ms}^2\lambda_{\max}(R_{mi}) + \frac{1}{2}\hat{d}_{sm}^2\lambda_{\max}(R_{si}) + \frac{1}{2}\hat{d}_i^2\lambda_{\max}(R_i) + \hat{d}_i^2\lambda_{\max}(P_{1i}) + (\hat{d}_r - \check{d}_r)^2\lambda_{\max}(P_{2i})) + \sum_{r=1}^{N}(\lambda_{\max}(Z_r) + (\hat{d}_r - \check{d}_r)\lambda_{\max}(U_r) + \frac{1}{2}\hat{d}_r^2\lambda_{\max}(Q_r) + \hat{d}_i^2\lambda_{\max}(P_{3r}) + (\hat{d}_r - \check{d}_r)^2\lambda_{\max}(P_{4r})) \le \varpi$ holds. Then a maximized estimate of DOA is obtained as $\delta_{\max} = 1/\sqrt{\varpi}$.

IV. SIMULATION AND EXPERIMENT RESULTS

This section gives the simulation and experiment results to verify the effectiveness of the proposed consensus controllers.

A. SIMULATION ON A SINGLE-MASTER-MULTI-SLAVE TCPS

In the simulation, a single-master-multi-slave TCPS consists of seven 3-DOF manipulators (i.e., one master robot and six slave robots), and the model is given as

$$M_m(q_m)\ddot{q}_m + C_m(q_m, \dot{q}_m)\dot{q}_m + G_m(q_m) = \tau_m - F_h$$
$$M_i(q_i)\ddot{q}_i + C_i(q_i, \dot{q}_i)\dot{q}_i + G_i(q_i) = \tau_i + F_i$$

whose components of motion dynamics are given in [31] and [32] and $i \in \{1, 2, 3, 4, 5, 6\}$. For clear illustration, model parameters of an arbitrary manipulator 1 are given as follows. Define $q_1 = [q_{11}, q_{12}, q_{13}]^T$, $G_1 = [G_{11}, G_{12}, G_{13}]^T$, $\tau_1 = [\tau_{11}, \tau_{12}, \tau_{13}]^T$ and $F_1 = [F_{11}, F_{12}, F_{13}]^T$, then model of PhantomTM robotic system is given as

$$\begin{bmatrix} m_{11} & m_{12} & m_{13} \\ m_{21} & m_{22} & m_{23} \\ m_{31} & m_{32} & m_{33} \end{bmatrix} \begin{bmatrix} \ddot{q}_{11} \\ \ddot{q}_{12} \\ \ddot{q}_{13} \end{bmatrix} + \begin{bmatrix} c_{11} & c_{12} & c_{13} \\ c_{21} & c_{22} & c_{23} \\ c_{31} & c_{32} & c_{33} \end{bmatrix} \times \begin{bmatrix} \dot{q}_{11} \\ \dot{q}_{12} \\ \dot{q}_{13} \end{bmatrix} = \begin{bmatrix} \tau_{11} \\ \tau_{12} \\ \tau_{13} \end{bmatrix} + \begin{bmatrix} F_{11} \\ F_{12} \\ F_{13} \end{bmatrix} - \begin{bmatrix} G_{11} \\ G_{12} \\ G_{13} \end{bmatrix}$$

where $m_{11} = \theta_1 + \theta_2\cos^2 q_{12} + (\theta_3 + \theta_5)\sin^3 q_{13} + 2\theta_6\cos q_{12}\sin q_{13}$, $m_{12} = 0$, $m_{13} = 0$, $m_{21} = 0$, $m_{22} = \theta_4 + \theta_5 - 2\sin(q_{12} - q_{13})$, $m_{31} = 0$, $m_{23} = m_{32} = \theta_5 - \theta_6 - 2\sin(q_{12} - q_{13})$, $m_{33} = \theta_5$, $c_{11} = -(\theta_2\sin q_{12}\cos q_{12} + \theta_6\sin q_{12}\sin q_{13})\dot{q}_{12} + ((\theta_3 + \theta_5)\sin q_{13}\cos q_{13} + \theta_6\cos q_{12}\cos q_{13})\dot{q}_{13}$, $c_{12} = -(\theta_2\sin q_{12}\cos q_{12} + \theta_6\sin q_{12}\sin q_{13})\dot{q}_{11}$, $c_{13} = ((\theta_3 + \theta_5)\sin q_{13}\cos q_{13} + \theta_6\cos q_{12}\cos q_{13})\dot{q}_{11}$, $c_{21} = (\theta_2\sin q_{12}\cos q_{12} + \theta_6\sin q_{12}\sin q_{13})\dot{q}_{11}$, $c_{22} = \theta_6\cos(q_{12} - q_{13})(\dot{q}_{13} - \dot{q}_{12})$, $c_{23} = \theta_6\cos(q_{12} - q_{13})(\dot{q}_{12} - \dot{q}_{13})$, $c_{31} = -(\theta_3 + \theta_5)\sin q_{13}\cos q_3\dot{q}_{11} - \theta_6\cos q_{12}\cos q_{13}\dot{q}_{11}$, $c_{32} = 0$, $c_{33} = 0$,

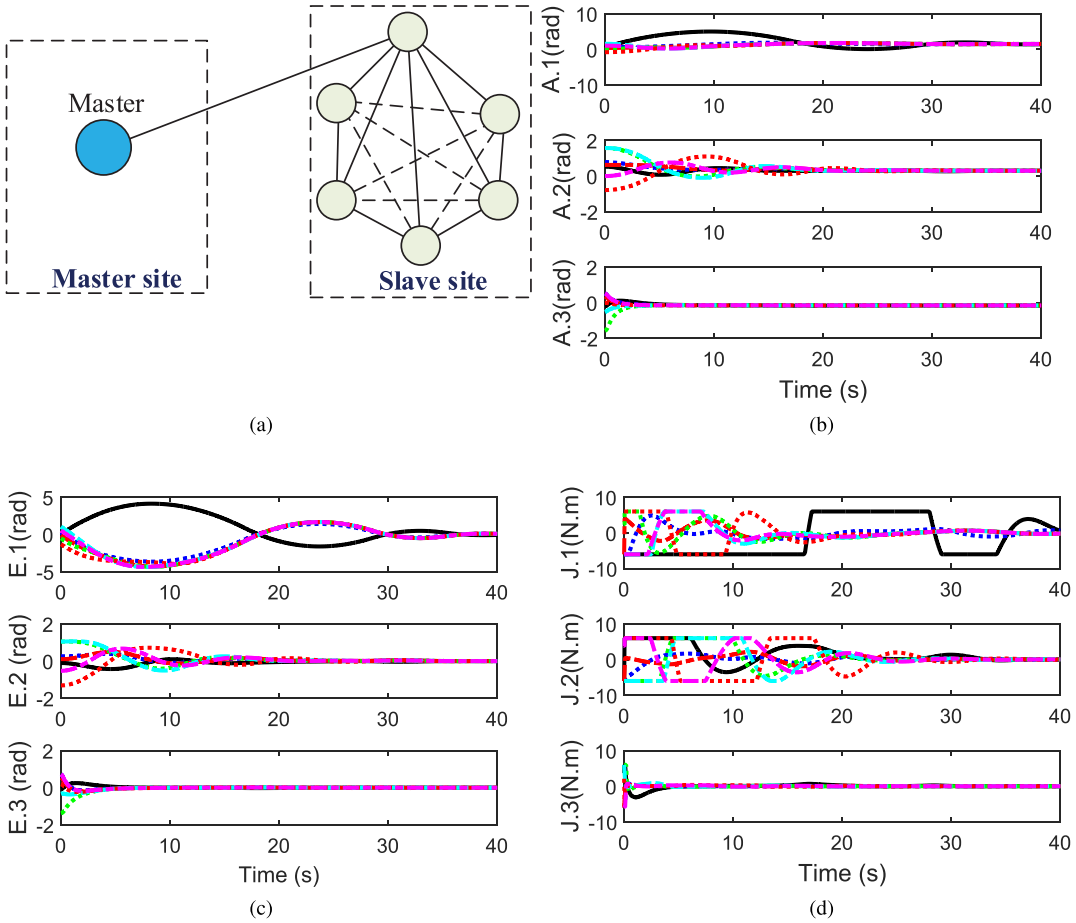

FIGURE 6. Simulation results for the decentralized consensus controller (14) under neighbor rule modes. (a) Communication topology of master and slaves. (b) Angles of manipulators. (c) Consensus errors of angles. (d) Control torque for manipulators.

$G_1 = 0$, $G_2 = \theta_7 \cos q_{12}$ and $G_3 = \theta_8 \sin q_{13}$. In special, $\theta_1 = 32$, $\theta_2 = 34$, $\theta_3 = 20$, $\theta_4 = 74$, $\theta_5 = 1$, $\theta_6 = 2$, $\theta_7 = -926$ and $\theta_8 = -685$.

Some parameters used for the simulation are designed as follows: $K_m = K_i = \alpha_m = \alpha_i = \text{diag}\{30, 30, 30\}$, and the saturation level is ± 6 for $i \in \{1, 2, 3, 4, 5, 6\}$. The single-way forward and backward time delays are chosen to be random variables with uniform distributions. The initial conditions for master and slave robots are given as: $q_m = (\pi/6, \pi/6, -0.2)^T$, $q_1 = (0, \pi/2, -\pi/2)^T$, $q_2 = (\pi/4, \pi/4, \pi/6)^T$, $q_3 = (\pi/8, \pi/5, \pi/9)^T$, $q_4 = (\pi/2, \pi/2, -\pi/6)^T$, $q_5 = (-\pi/4, -\pi/4, 0)^T$, $q_6 = (\pi/3, 0, \pi/6)^T$, $\dot{q}_m = (1, 0, 0)^T$ and $\dot{q}_m = \dot{q}_i = (0, 0, 0)^T$ for $i \in \{1, 2, 3, 4, 5, 6\}$. Human operator exerts forces $F = [F_x, F_y, F_z]^T$ on the master, where F_x, F_y and F_z are the force components in X-axis, Y-axis and Z-axis, respectively. The human exerted forces F are designed as: $F_x = 20t - 10$, if $t \in [0.5, 1)$; $F_x = 10$, if $t \in [1, 2)$; $F_x = -20t + 50$, if $t \in [2, 2.5)$; $F_x = 0$, if $t \in [0, 0.5) \cup [2.5, 40]$; $F_y = 20t - 30$, if $t \in [1.5, 2)$; $F_y = 10$, if $t \in [2, 3)$; $F_y = -20t + 70$, if $t \in [3, 3.5)$; $F_y = 0$, if $t \in [0, 1.5) \cup [3, 40]$; $F_z = 0$, if $t \in [0, 40]$.

We first investigate the performance of centralized consensus controller (4). With the centralized mode (e.g., [13], [21], [22]), the communication topology of master and slave robots is shown in Fig. 5 (a). It can be seen that each slave robot bilaterally communicates with the master robot, while there is no cooperation among slave robots. Under the centralized topology relationship, we adopt centralized consensus controller (4) to drive the states of master and slave robots. With the centralized consensus controller, angles of manipulators, i.e., q_m, q_1, q_2, q_3, q_4, q_5 and q_6, are shown in Fig. 5(b). Consensus errors of angles, i.e., $q_m - q_1$, $q_1 - q_m$, $q_2 - q_m$, $q_3 - q_m$, $q_4 - q_m$, $q_5 - q_m$ and $q_6 - q_m$, are shown in Fig. 5(c). Clearly, state consensus can be achieved because all the consensus errors approximately converge to the value of zero. Moreover, the control torques for master and slave robots with the centralized consensus controller are provided by Fig. 5 (d). When the sufficient stability conditions are satisfied for the centralized consensus controller (4), it can be shown that control torques in Fig. 5(d) are smooth,and they are restricted by the saturation bounds.

In the following, we investigate the performance of decentralized consensus controller (14). As mentioned above,

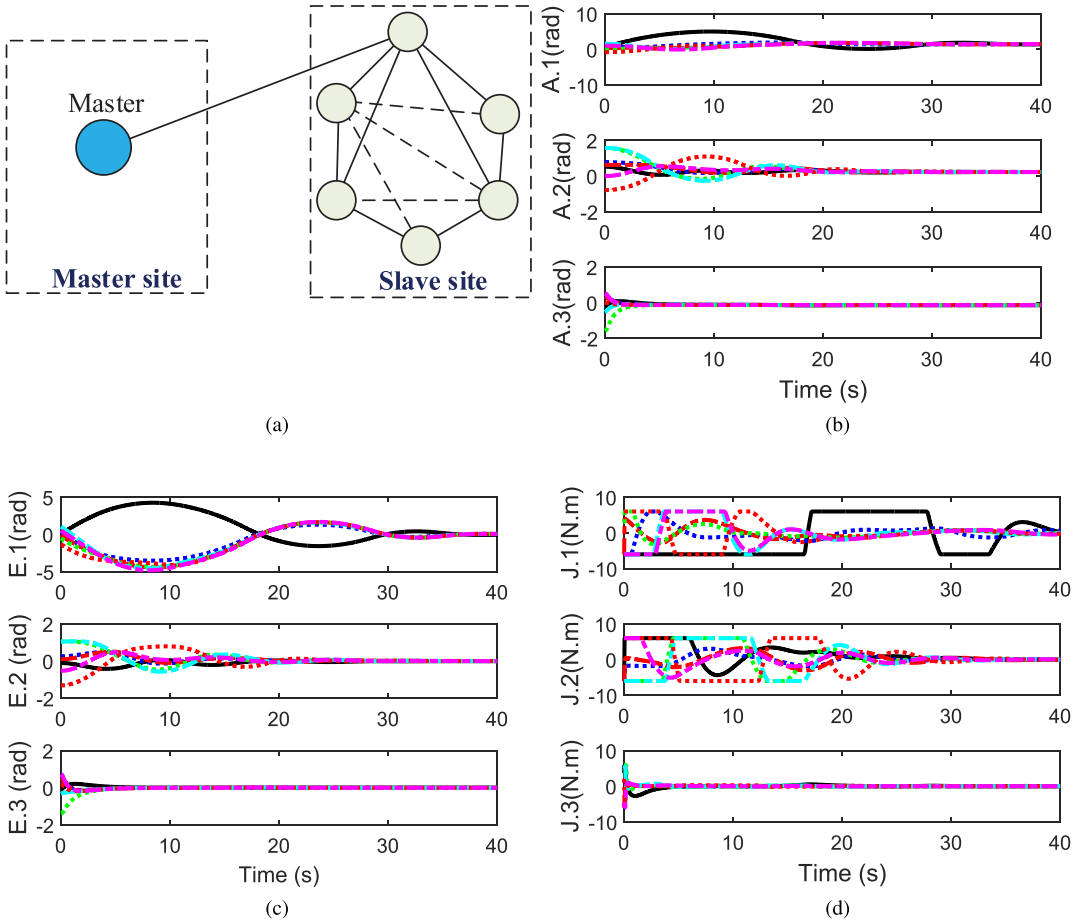

FIGURE 7. Simulation results for the decentralized consensus controller (14) under the optimized topology in this paper. (a) Communication topology of master and slaves. (b) Angles of manipulators. (c) Consensus errors of angles. (d) Control torque for manipulators.

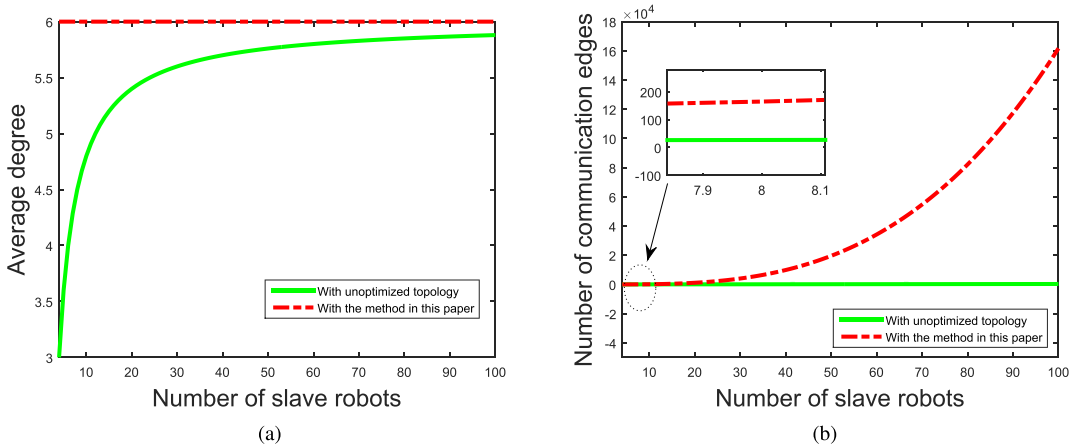

FIGURE 8. Comparison between the unoptimized topology in [18] and [24]) and the optimized topology in this paper. (a) Average degree for each slave robot. (b) Number of communication edges in slave site.

the neighbor rule-based network topology can increase some unnecessary interactions, and the redundancy makes the communication complex and inefficient. Fig. 6(a) shows the topology relationships of the slave robots in *neighbor rule* decentralized modes (e.g., [18], [24]). With the unoptimized topology, we use the decentralized controller (14) to achieve state consensus. The angles of manipulators, i.e., q_m, q_1, q_2, q_3, q_4, q_5 and q_6, are shown in Fig. 6(b). Consensus errors of

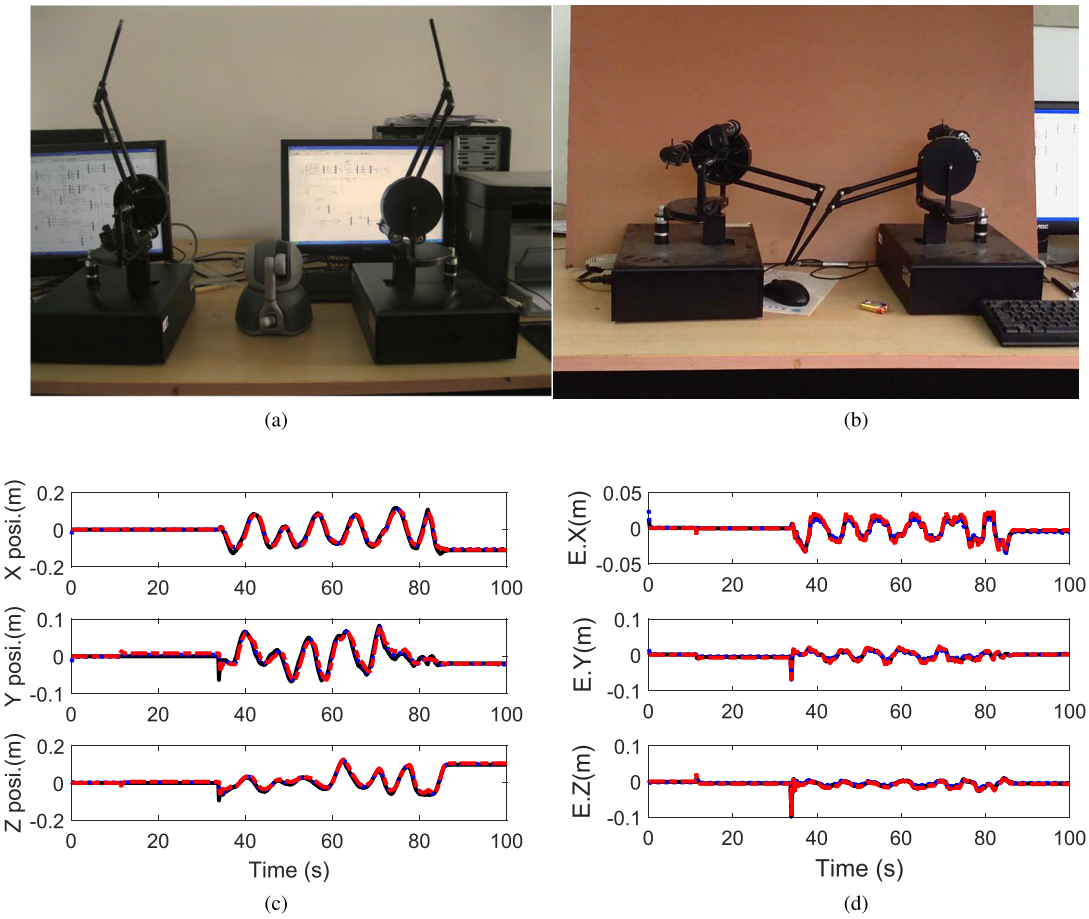

FIGURE 9. Experimental results, where real, dotted and dashed lines denote the relevant states for master, slave 1 and slave 2, respectively. (a) Experimental setup. (b) Consensus of robots. (c) Position trajectories. (d) Position errors.

angles, i.e., $q_m - q_1$, $q_1 - q_m$, $q_2 - q_m$, $q_3 - q_m$, $q_4 - q_m$, $q_5 - q_m$ and $q_6 - q_m$, are shown in Fig. 6 (c). Clearly, consensus can be achieved because consensus errors approximately converge to zero. Fig. 6(d) shows the control torques, and control torques are smooth while being restricted by the saturation bounds.

When Algorithm 1 is adopted to optimize the network topology, we can obtain the optimized topology of master and slave robots, as shown in Fig. 7(a). Obviously, communication complexity in this paper is the least, as the communicate links in this paper is 12, while Fig. 6 (a) 15. With the optimized min-weighted rigid graph, we use the decentralized controller (14) to achieve state consensus. The angles of manipulators are shown in Fig. 7(b), and the consensus errors of angles are shown in Fig. 7(c). Similar to the unoptimized network topology, consensus can be guaranteed as all consensus errors approximately converge to the value of zero. Control torques for master and slaves with the centralized consensus controller are provided by Fig. 7(d). When the sufficient stability conditions are satisfied for our controllers, it can be shown that control torques in Fig. 7(d) are smooth, and they are restricted by the saturation bounds. Notice that the topologies in centralized and decentralized modes are different, and this characteristic leads to the differences of stress points for human operator. Thus, the final convergence values are different with the centralized and decentralized modes. As our objective is to ensure the state consensus of master and slave robots, thereby the difference of final convergence values does not affect the whole performance of state consensus for multi-slave TCPS.

Finally, we give the comparison results. Fig. 8(a) shows the average degree for each slave robot, and the degree in unoptimzied topology is fixed as 6. It can be seen that the degree in this paper converges to 6 with the number increasing of slave robots, i.e., the degree in this paper can meet the demand of connectivity maintenance. In Fig. 8(b), the number of communication edges in slave site is given. It can be seen that the topology in this paper can reduce some redundancy links by comparing with the unoptimized topology.

B. EXPERIMENT ON A MULTI-SLAVE TCPS

Experimental results are presented in this section. The experiment platform is composed of three Phantom Premium 1.5HF robotic arms, i.e., one master robot and two slave robots with 3-DOF positional sensing. This platform is

provided by SensAble Technologies, Inc, which is shown in Fig. 9(a). In this section, we only check the effectiveness of the proposed centralized consensus controller, due to the limited number of slave robots in our lab.

In the communication channel, the time delays between master and slave robots are deigned to be random variables, which are with uniform distributions. Master robot is operated by human operator to obtain the desired state trajectory, and two slave robots are enforced to track the trajectory of master robot. With the Jacobian coordinate transformation, the experiment is transformed from angles to position space.

Under the consensus tracking controller (4), the two slave robots can effectively track the trajectory of the master robot as shown by Fig. 9(b). To show more clearly, Fig. 9(c) show the position trajectories of master and slave robot. In addition, position errors during the consensus process are shown in Fig. 9(d). Obviously, consensus task is achieved, because all the states errors approximately converge to zero.

V. CONCLUSION AND FUTURE WORKS

In this paper, we investigate the consensus problem for delayed single-master-multi-slave TCPS in the presence of actuator saturation. To achieve consensus task, centralized and decentralized consensus controllers are respectively designed for TCPS, such that the master robot can track the slave robots while each slave robot keeps state consensus with the master robot. Stability conditions are given to illustrate that the consensus tracking controller can stabilize the TCPS. We also give a min-weighted rigid graph based topology optimization scheme to simplify the information fusion in decentralized controller design. Finally, simulation and experiment results are performed to show the validity of our proposed methods.

In future, more complex environments will considered, such as the consensus control in underwater environment. Moreover, how to describe the time delay in underwater environment is also our future work.

APPENDIX A
NOTATIONS FOR THEOREM 1

$$\begin{aligned}\Gamma_\delta &= (\hat{\varrho}_m + \sum_{r=1}^{N}\frac{1}{2}\hat{d}_{ms}^2\lambda_{\max}(R_{mr}))\delta_{m1}^2 + \sum_{r=1}^{N}\hat{\varrho}_r\delta_{sr1}^2 \\ &\quad + \sum_{r=1}^{N}\frac{1}{2}\hat{d}_{sm}^2\lambda_{\max}(R_{sr})\delta_{sr1}^2 + \sum_{r=1}^{N}(\lambda_{\max}(W_r) \\ &\quad + (\hat{d}_r - \check{d}_r)\lambda_{\max}(S_r) + \hat{d}_r^2\lambda_{\max}(P_1) + (\hat{d}_r - \check{d}_r)^2 \\ &\quad \times \lambda_{\max}(P_2))\delta_{er1}^2 + \sum_{r=1}^{N}\frac{1}{2}\hat{d}_r^2\lambda_{\max}(R_r)\delta_{er2}^2.\end{aligned}$$

$$\Phi = \Phi_0 - \sum_{r=1}^{N}\frac{1}{\hat{d}_i}\Gamma_r^T\Phi_{1r}\Gamma_r,$$

$$\begin{aligned}\Phi_0 &= \hat{W} + \hat{S} + \hat{R}_m + \hat{R}_s + \hat{R} \\ &\quad + \sum_{r=1}^{N}(\hat{N}_r + \hat{M}_r + \hat{N}_r^T + \hat{M}_r^T) + J_0^T P_1 J_1 \\ &\quad + J_1^T P_1 J_0 + J_2^T P_2 J_3 + J_3^T P_2 J_2 + \Phi_3\hat{W} \\ &= \left[0_{n(10N+1)\times n(3N+1)}\ 2\tilde{w}_1\ 0_{n(10N+1)\times n(3N+1)}\right]\end{aligned}$$

with $\tilde{w}_1 = col\{\varpi, -2W_1\tilde{e}_1, \ldots, -2W_N\tilde{e}_N, 0_{9nN\times nN}\}$ and $\tilde{e}_r^T$ is block entry matrix such as $\tilde{e}_2 = \left[0, I, 0, \cdots, 0\right]_{n\times nN}$, $\hat{S} = \mathrm{diag}\{0_{n(4N+1)}, (1-\dot{d}_1(t))S_1, \cdots, (1-\dot{d}_N(t))S_N, -S_1, \cdots, -S_N, 0_{4nN}\}$ and $\hat{R}_m = \mathrm{diag}\{\sum_{r=1}^{N}\hat{d}_{ms}R_{mr}, 0_{nN}, -\frac{R_{m1}}{\hat{d}_{ms}}, \cdots, -\frac{R_{mN}}{\hat{d}_{ms}}, 0_{8nN}\}$, where diag{...} denotes a block-diagonal matrix,

$$\begin{aligned}\hat{R}_s &= \mathrm{diag}\{0_n, \hat{d}_{sm}R_{s1}, \cdots, \hat{d}_{sm}R_{sN}, 0_{nN}, -\frac{1}{\hat{d}_{sm}}R_{s1}, \cdots, \\ &\qquad -\frac{1}{\hat{d}_{sm}}R_{sN}, 0_{7nN}\}, \\ \hat{R} &= \begin{bmatrix}\sum_{r=1}^{N}\hat{d}_rR_r & \sum_{r=1}^{N}\hat{d}_rR_r\tilde{e}_r & 0_{n\times 9nN} \\ 0_{N\times n} & \mathrm{diag}\{\hat{d}_1R_1, \ldots \hat{d}_NR_N\} & 0_{nN\times 9nN} \\ 0_{9nN\times n} & 0_{n\times nN} & 0_{9nN\times 9nN}\end{bmatrix} \\ \hat{N}_r &= N_rJ_{2r}, \hat{M}_r = M_rJ_{3r} \\ J_{2r} &= \left[0_{n\times n(3N+1)}\ -\tilde{e}_r\ \tilde{e}_r\ 0_{n\times 3nN}\ -\tilde{e}_r\ 0_{n\times nN}\right] \\ J_{3r} &= \left[0_{n\times n(4N+1)}\ \tilde{e}_r\ -\tilde{e}_r\ 0_{n\times 3nN}\ -\tilde{e}_r\right] \\ J_0 &= \left[0_{nN\times n(3N+1)}\ \tilde{j}_1\ -\tilde{j}_2\ 0_{nN\times 5nN}\right], \\ J_1 &= \left[0_{nN\times n(6N+1)}\ \tilde{j}_3\ 0_{nN\times 3nN}\right], \\ J_2 &= \left[0_{nN\times n(4N+1)}\ \tilde{j}_2\ -\tilde{j}_1\ 0_{nN\times 4nN}\right], \\ J_3 &= \left[0_{nN\times n(7N+1)}\ \tilde{j}_4\ 0_{nN\times 2nN}\right]\end{aligned}$$

with $\tilde{j}_1 = col\{\tilde{e}_1, \cdots, \tilde{e}_N\}, \tilde{j}_2 = col\{(1-\dot{d}_1(t))\tilde{e}_1, \ldots, (1-\dot{d}_N(t))\tilde{e}_N\}, \tilde{j}_3 = col\{d_1(t)\tilde{e}_1, \cdots, d_N(t)\tilde{e}_N\}, \tilde{j}_4 = col\{(\hat{d}_1 - d_1(t))\tilde{e}_1, \cdots, (\hat{d}_N - d_N(t))\tilde{e}_N\}$, where col(·) stands for a column vector by stacking them together. Φ_3, as shown at the top of the next page.

with $\tilde{\varphi}_1 = \frac{1}{N}\sum_{r=1}^{N}[(-D_i\alpha_m + D_i^-H_{\alpha m}) + (-D_i\alpha_m + D_i^-H_{\alpha m})^T\}$, $\tilde{\varphi}_2 = col\{[(-D_i\alpha_1 + D_i^-H_{\alpha 1}) + (-D_i\alpha_1 + D_i^-H_{\alpha 1})]^T\tilde{e}_1, \cdots, [(-D_i\alpha_N + D_i^-H_{\alpha N}) + (-D_i\alpha_N + D_i^-H_{\alpha N})]^T\tilde{e}_N\}$, $\tilde{\varphi}_3 = col\{(D_ik_1 + D_i^-H_{k1})\tilde{e}_1, \cdots, (D_ik_N + D_i^-H_{kN})\tilde{e}_N\}$, $\tilde{\varphi}_4 = \frac{1}{N}(-D_iK_m + D_i^-H_{km})\bar{I}_{n\times nN}$.

$$\begin{aligned}\Gamma_r^T &= \left[\Gamma_{1r}^T\ \Gamma_{2r}^T\ \Gamma_{3r}^T\ \Gamma_{4r}^T\right]^T, \\ \Gamma_{1r} &= [0_{n(9N+1)\times n}, \tilde{e}_r], \\ \Gamma_{2r} &= [0_{n\times n(4N+1)}, \tilde{e}_r, \tilde{e}_r, \quad 0_{n\times nN}, f_r, 0_{n\times 2nN}], \\ \Gamma_{3r} &= \left[0_{n\times n(8N+1)}, \tilde{e}_r, 0_{n\times nN}\right], \\ \Gamma_{4r} &= [0_{n\times n(3N+1)}, \quad \tilde{e}_r, \tilde{e}_r, 0_{n\times nN}, f_r, 0_{n\times 3nN}].\end{aligned}$$

$f_r = [0, \cdots, -2I, \cdots, 0]_{n\times nN}$ such as $f_2 = [0, -2I, 0, \cdots, 0]_{n\times nN}$, $\tilde{R}_r = \mathrm{diag}\{R_r, 3R_r\}$, $Q = \mathrm{diag}\{\hat{\varrho}_mI, \hat{\varrho}_1I, \cdots, \hat{\varrho}_NI, W_1, \cdots, W_N\}$

APPENDIX B
NOTATIONS FOR THEOREM 3

$$\begin{aligned}\hat{\Phi} &= \bar{\Phi} - \sum_{i=1}^{N}\frac{b_i}{\hat{d}_i}\Theta^T\breve{R}_i\Theta - \sum_{i=1}^{N}\sum_{j=1}^{N}\frac{a_{ij}}{\hat{d}_i}\Xi^T\breve{Q}_i\Xi + N_i\Pi_1 \\ &\quad + \Pi_1^TN_i^T + M_i\Pi_2 + \Pi_2^TM_i^T + G_i\Pi_3 + \Pi_3^TG_i^T \\ &\quad + H_i\Pi_4 + \Pi_4^TH_i^T. \\ \Theta^T &= [\Theta_1^T, \Theta_2^T, \Theta_3^T, \Theta_4^T]\end{aligned}$$

$$\Phi_3 = \begin{bmatrix} \tilde{\varphi}_1 & 0_{n\times nN} & 0_{n\times nN} & \tilde{\varphi}_4 & \tilde{\varphi}_4 & 0_{n\times 6nN} \\ 0_{nN\times n} & \tilde{\varphi}_2 & -\tilde{\varphi}_3 & 0_{nN\times nN} & & \\ 0_{9nN\times n} & 0_{9nN\times nN} & 0_{9nN\times nN} & 0_{9nN\times nN} & 0_{9nN\times nN} & 0_{9nN\times nN} \end{bmatrix}$$

with

$$\begin{aligned}
\Theta_1 &= [0_{n\times\ (1+N+7\bar{\Im}_m+3\sum_{i=1}^{N}\bar{\Im}_i)n}, [e_i^i]_{n\times\bar{\Im}_m n}, \\
&\qquad 0_{n\times\ (\bar{\Im}_m+4\sum_{i=1}^{N}\bar{\Im}_i)n}], \\
\Theta_2 &= [0_{n\times\ (1+N+2\bar{\Im}_m)n}, [e_i^i]_{n\times\bar{\Im}_m n}, [e_i^i]_{n\times\bar{\Im}_m n}, \\
&\quad 0_{n\times\ (\bar{\Im}_m+3\sum_{i=1}^{N}\bar{\Im}_i)n}, -2[e_i^i]_{n\times\bar{\Im}_m n}, 0_{n\times\ (3\bar{\Im}_m+4\sum_{i=1}^{N}\bar{\Im}_i)n}], \\
\Theta_3 &= [0_{n\times\ (1+N+8\bar{\Im}_m+3\sum_{i=1}^{N}\bar{\Im}_i)n}, [e_i^i]_{n\times\bar{\Im}_m n}, 0_{n\times 4\sum_{i=1}^{N}\bar{\Im}_i n}], \\
\Theta_4 &= [0_{n\times\ (1+N+3\bar{\Im}_m)n}, [e_i^i]_{n\times\bar{\Im}_m n}, [e_i^i]_{n\times\bar{\Im}_m n}, \\
&\quad 0_{n\times\ (\bar{\Im}_m+3\sum_{i=1}^{N}\bar{\Im}_i)n}, -2[e_i^i]_{n\times\bar{\Im}_m n}, 0_{n\times\ (2\bar{\Im}_m+4\sum_{i=1}^{N}\bar{\Im}_i)n}]. \\
\Xi^T &= [\Xi_1^T, \Xi_2^T, \Xi_3^T, \Xi_4^T]
\end{aligned}$$

with

$$\begin{aligned}
\Xi_1 &= [0_{n\times\ (1+N+9\bar{\Im}_m+5\sum_{i=1}^{N}\bar{\Im}_i)n}, [e_i^i]_{n\times\sum_{i=1}^{N}\bar{\Im}_i n}, 0_{n\times\sum_{i=1}^{N}\bar{\Im}_i n}], \\
\Xi_2 &= [0_{n\times\ (1+N+5\bar{\Im}_m)n}, [e_i^i]_{n\times\sum_{i=1}^{N}\bar{\Im}_i n}, [e_i^i]_{n\times\sum_{i=1}^{N}\bar{\Im}_i n}, \\
&\quad 0_{n\times\ (4\bar{\Im}_m+\sum_{i=1}^{N}\bar{\Im}_i)n}, -2[e_i^i]_{n\times\sum_{i=1}^{N}\bar{\Im}_i n}, 0_{n\times 3\sum_{i=1}^{N}\bar{\Im}_i n}], \\
\Xi_3 &= [0_{n\times\ (1+N+9\bar{\Im}_m+6\sum_{i=1}^{N}\bar{\Im}_i)n}, [e_i^i]_{n\times\sum_{i=1}^{N}\bar{\Im}_i n}], \\
\Xi_4 &= [0_{n\times\ (1+N+5\bar{\Im}_m+\sum_{i=1}^{N}\bar{\Im}_i)n}, [e_i^i]_{n\times\sum_{i=1}^{N}\bar{\Im}_i n}, [e_i^i]_{n\times\sum_{i=1}^{N}\bar{\Im}_i n}, \\
&\quad 0_{n\times\ (4\bar{\Im}_m+\sum_{i=1}^{N}\bar{\Im}_i)n}, -2[e_i^i]_{n\times\sum_{i=1}^{N}\bar{\Im}_i n}, 0_{n\times 2\sum_{i=1}^{N}\bar{\Im}_i n}]. \\
\Pi_1 &= [0_{n\times\ (1+N+2\bar{\Im}_m)n}, [e_i^i]_{n\times\bar{\Im}_m n}, -[e_i^i]_{n\times\bar{\Im}_m n}, \\
&\quad 0_{n\times\ (3\bar{\Im}_m+3\sum_{i=1}^{N}\bar{\Im}_i)n}, -[e_i^i]_{n\times\bar{\Im}_m n}, 0_{n\times\ (\bar{\Im}_m+5\sum_{i=1}^{N}\bar{\Im}_i)n}], \\
\Pi_2 &= [0_{n\times\ (1+N+3\bar{\Im}_m)n}, [e_i^i]_{n\times\bar{\Im}_m n}, -[e_i^i]_{n\times\bar{\Im}_m n}, \\
&\quad 0_{n\times\ (3\bar{\Im}_m+3\sum_{i=1}^{N}\bar{\Im}_i)n}, -[e_i^i]_{n\times\bar{\Im}_m n}, 0_{n\times 4\sum_{i=1}^{N}\bar{\Im}_i n}], \\
\Pi_3 &= [0_{n\times\ (1+N+5\bar{\Im}_m)n}, [e_i^i]_{n\times\sum_{i=1}^{N}\bar{\Im}_i n}, -[e_i^i]_{n\times\sum_{i=1}^{N}\bar{\Im}_i n}, \\
&\quad 0_{n\times\ (4\bar{\Im}_m+3\sum_{i=1}^{N}\bar{\Im}_i)n}, -[e_i^i]_{n\times\sum_{i=1}^{N}\bar{\Im}_i n}, 0_{n\times\sum_{i=1}^{N}\bar{\Im}_i n}], \\
\Pi_4 &= [0_{n\times\ (1+N+5\bar{\Im}_m)n}, [e_i^i]_{n\times\sum_{i=1}^{N}\bar{\Im}_i n}, -[e_i^i]_{n\times\sum_{i=1}^{N}\bar{\Im}_i n}, \\
&\quad 0_{n\times\ (4\bar{\Im}_m+3\sum_{i=1}^{N}\bar{\Im}_i)n}, -[e_i^i]_{n\times\sum_{i=1}^{N}\bar{\Im}_i n}],
\end{aligned}$$

where $[e_i^i]_{n\times\bar{\Im}_m n}$ is block entry matrix such as $[e_2^i]_{n\times\bar{\Im}_m n} = [0\ I\ 0_{n\times\ (\bar{\Im}_m-2)n}]$, $\Im_m$ is the set of neighbours of master and $\bar{\Im}_m$ is the number of neighbours of master.

$$\breve{R}_i = \begin{bmatrix} R_i & 0 & X_{11}^i & X_{12}^i \\ 0 & 3R_i & X_{21}^i & X_{22}^i \\ X_{11}^{iT} & X_{12}^{iT} & R_i & 0 \\ X_{21}^{iT} & X_{22}^{iT} & 0 & 3R_i \end{bmatrix},$$

$$\breve{Q}_i = \begin{bmatrix} Q_i & 0 & Y_{11}^i & Y_{12}^i \\ 0 & 3Q_i & Y_{21}^i & Y_{22}^i \\ Y_{11}^{iT} & Y_{12}^{iT} & Q_i & 0 \\ Y_{21}^{iT} & Y_{22}^{iT} & 0 & 3Q_i \end{bmatrix}.$$

The terms of $\bar{\Phi}$ are $\bar{\Phi}_{1,1} = (-D_r\alpha_m + D_r^- H_{\alpha m}) + \sum_{i=1}^{N} b_i(\hat{d}_i R_i + \hat{d}_{ms} R_{mi}) + (-D_r\alpha_m + D_r^- H_{\alpha m})^T$, $\bar{\Phi}_{1,2} = [\epsilon_1\ \ldots\ \epsilon_N]_{n\times Nn}$ with $\epsilon_i = b_i\hat{d}_i R_i$, if $i \in \Im_m$; $\epsilon_i = 0$, otherwise,

$$\begin{aligned}
\bar{\Phi}_{1,4} &= [b_{i_1}(-D_rK_m + D_r^- H_{km}), \ldots, b_{i_{\bar{\Im}_m}} \\
&\qquad (-D_rK_m + D_r^- H_{km})]_{n\times\bar{\Im}_m n}, \\
\bar{\Phi}_{1,5} &= [b_{i_1}(-D_rK_m + D_r^- H_{km} + W_{i_1}), \ldots, b_{i_{\bar{\Im}_m}} \\
&\qquad (-D_rK_m + D_r^- H_{km} + W_{i_{\bar{\Im}_m}})]_{n\times\bar{\Im}_m n}, \\
\bar{\Phi}_{6,6} &= \mathrm{diag}\{b_{i_v}(1-\dot{d}_{i_v}(t))W_{i_v}\}_{\bar{\Im}_m n\times\bar{\Im}_m n}, \\
\bar{\Phi}_{7,7} &= \mathrm{diag}\{-b_{i_v}W_{i_v}\}_{\bar{\Im}_m n\times\bar{\Im}_m n}, \\
\bar{\Phi}_{5,11} &= \mathrm{diag}\{d_{iv}(t)b_{iv}P_{1iv}\}_{\bar{\Im}_m n\times\bar{\Im}_m n}, \\
\bar{\Phi}_{6,11} &= \mathrm{diag}\{-(1-\dot{d}_{i_v}(t))d_{i_v}(t)b_{iv}P_{1i_v}\}_{\bar{\Im}_m n\times\bar{\Im}_m n}, \\
\bar{\Phi}_{6,12} &= \mathrm{diag}\{(1-\dot{d}_{iv}(t))(\hat{d}_{i_v} - d_{i_v}(t))b_{i_v}P_{2i_v}\}_{\bar{\Im}_m n\times\bar{\Im}_m n}, \\
\bar{\Phi}_{7,12} &= \mathrm{diag}\{(\hat{d}_{i_v} - d_{i_v}(t))b_{i_v}P_{2i_v}\}_{\bar{\Im}_m n\times\bar{\Im}_m n}, \\
\bar{\Phi}_{3,3} &= \mathrm{diag}\{-R_{mi_v}b_{i_v}/\hat{d}_{ms}\}_{\bar{\Im}_m n\times\bar{\Im}_m n}, \\
\bar{\Phi}_{4,4} &= \mathrm{diag}\{-R_{si_v}b_{i_v}/\hat{d}_{sm}\}_{\bar{\Im}_m n\times\bar{\Im}_m n},
\end{aligned}$$

where the subscript $i_v \in \{1, 2, \ldots, N | b_{i_v} \neq 0\}$, $v = 1, 2, \ldots, \bar{\Im}_m$, and i_{v+1} is the smallest integer lager than i_v, i.e., $i_{v+1} = \mathrm{ceil}(i_v)$.

$$\begin{aligned}
\bar{\Phi}_{2,2} &= \mathrm{diag}\{-D_r\alpha_i + D_r^- H_\alpha + \iota_i + \sum_{j=1}^{N} a_{ij}Q_i \\
&\qquad + \sum_{j=1}^{N} a_{ji}Q_i\}_{N\times N} + \Lambda_{N\times N}, \quad i = 1, 2, \ldots, N, \\
&\qquad \iota_i = b_i(\hat{d}_{sm}R_{si} + \hat{d}_i R_i),
\end{aligned}$$

if $i \in \Im_m$, and 0 otherwise, $\Lambda = [\varkappa_{1,1}, \ldots, \varkappa_{1,N}; \ldots; \varkappa_{N,1}, \ldots, \varkappa_{N,N}]$ with $\varkappa_{p,v} = -a_{vp}Q_v$, if $p \in \Im_v$, and 0 otherwise, $\bar{\Phi}_{2,3} = [\varphi_{1,1}, \ldots, \varphi_{1,\bar{\Im}_m}; \ldots; \varphi_{N,1}, \ldots, \varphi_{N,\bar{\Im}_m}]_{Nn\times\bar{\Im}_m n}$ with $\varphi_{p,v} = -b_p(D_rK_p + D_r^- H_{kbp})$, if $p \in \{1, 2, \ldots, N | b_p \neq 0\}$, v is the number of neighbours of master from 1 to p; $\varphi_{p,v} = 0$ otherwise, $\bar{\Phi}_{2,5} = [\bar{\varphi}_{1,1}, \ldots, \bar{\varphi}_{1,\bar{\Im}_m}; \ldots; \bar{\varphi}_{N,1}, \ldots, \bar{\varphi}_{N,\bar{\Im}_m}]_{Nn\times\bar{\Im}_m n}$ with $\bar{\varphi}_{p,v} = -\varphi_{p,v} - b_p W_p$ if $p \in \{1, 2, \ldots, N | b_p \neq 0\}$, v is number of neighbours of master from 1 to p; $\bar{\varphi}_{p,v} = 0$, otherwise,

$$\bar{\Phi}_{2,8} = \begin{bmatrix} a_{1j_1^1}\breve{A}_1 \ldots a_{1j_{\bar{\Im}_1}^1}\breve{A}_1 0_{1\times\bar{\Im}_2} \ldots 0_{1\times\bar{\Im}_N} \\ 0_{1\times\bar{\Im}_1} a_{2j_1^2}\breve{A}_2 \ldots a_{2j_{\bar{\Im}_2}^2}\breve{A}_2 0_{1\times\bar{\Im}_3} \ldots 0_{1\times\bar{\Im}_N} \\ \vdots \\ 0_{1\times\bar{\Im}_1} \ldots 0_{1\times\bar{\Im}_{N-1}} a_{Nj_1^N}\breve{A}_N \ldots a_{Nj_{\bar{\Im}_N}^N}\breve{A}_N \end{bmatrix} + \Delta$$

with $\breve{A}_i = D_r K_1 + D_r^- H_{kai}$ and $i \in \{1, \ldots N\}$,

$$\Delta = \begin{bmatrix} [a_{1j}Z_1] & \ldots & \ldots & \varepsilon_{1,\sum_{i=1}^{N}\bar{\Im}_i} \\ \varepsilon_{2,1} & [a_{2j}Z_2] & \ldots & \vdots \\ \vdots & \vdots & \ddots & \vdots \\ \varepsilon_{N,1} & \ldots & \ldots & [a_{Nj}Z_N] \end{bmatrix}$$

and $\varepsilon_{p,v} = -a_{vp}Z_v$, if $p \in \Im_v$, and 0 otherwise,

$$\begin{aligned}
\bar{\Phi}_{9,9} &= \mathrm{diag}\{a_{vj_p^v}(1-\dot{d}_v(t))U_v\}_{\sum_{i=1}^{N}\bar{\Im}_i n \times \sum_{i=1}^{N}\bar{\Im}_i n}, \\
\bar{\Phi}_{10,10} &= \mathrm{diag}\{-a_{vj_p^v}U_v\}_{\sum_{i=1}^{N}\bar{\Im}_i n \times \sum_{i=1}^{N}\bar{\Im}_i n}, \\
\bar{\Phi}_{8,15} &= \mathrm{diag}\{a_{vj_p^v}d_v(t)P_{3v}\}_{\sum_{i=1}^{N}\bar{\Im}_i n \times \sum_{i=1}^{N}\bar{\Im}_i n}, \\
\bar{\Phi}_{9,15} &= \mathrm{diag}\{-a_{vj_p^v}(1-\dot{d}_v(t))d_v(t)P_{3v}\}_{\sum_{i=1}^{N}\bar{\Im}_i n \times \sum_{i=1}^{N}\bar{\Im}_i n}, \\
\bar{\Phi}_{9,16} &= \mathrm{diag}\{-a_{vj_p^v}(1-\dot{d}_v(t))(\hat{d}_v - d_v(t))P_{4v}\}_{\sum_{i=1}^{N}\bar{\Im}_i n \times \sum_{i=1}^{N}\bar{\Im}_i n}, \\
\bar{\Phi}_{10,16} &= \mathrm{diag}\{-a_{vj_p^v}(\hat{d}_v - d_v(t))P_{4v}\}_{\sum_{i=1}^{N}\bar{\Im}_i n \times \sum_{i=1}^{N}\bar{\Im}_i n},
\end{aligned}$$

where $j_p^v \in \{1, 2, \ldots, N | a_{vj_p^v} \neq 0\}, p = 1, 2, \ldots, \bar{\Im}_v, v = 1, 2, \ldots, N, j_{p+1}^v = \mathrm{ceil}(j_p^v)$, the other $\bar{\Phi}$ are zero.

$$\begin{aligned}
\Omega = \mathrm{diag}\{&\hat{\varrho}_m I, \hat{\varrho}_r I, b_{i_v} W_{i_v}, a_{rj_p^r} Z_{rj_p^r}\}, \\
& i_v \in \{1, 2, \ldots, N | b_{i_v} \neq 0\}, \quad v = 1, 2, \ldots, \bar{\Im}_m, \\
& i_{v+1} = ceil(i_v), \quad j_p^r \in \{1, 2, \ldots, N | a_{rjr} \neq 0\}, \\
& p = 1, 2, \ldots, \bar{\Im}_r, \quad r = 1, 2, \ldots, N, \\
& j_{p+1}^r = \mathrm{ceil}(j_p^r),
\end{aligned}$$

$$\begin{aligned}
\hat{\Gamma}_\delta = &(\hat{\varrho}_m + \frac{1}{2}\sum_{i=1}^{N} b_i \hat{d}_{ms}^2 \lambda_{\max}(R_{mi}))\delta_{m1}^2 \\
&+(\sum_{i=1}^{N}\hat{\varrho}_i + \frac{1}{2}\sum_{i=1}^{N} b_i \times \hat{d}_{sm}^2 \lambda_{\max}(R_{si}))\delta_{si1}^2 \\
&+ \sum_{i=1}^{N} b_i(\lambda_{\max}(W_i) + \hat{d}_i^2 \lambda_{\max}(P_{1i}) \\
&+ (\hat{d}_i - \breve{d}_i)^2 \lambda_{\max}(P_{2i}) + (\hat{d}_i - \breve{d}_i)\lambda_{\max}(S_i))\delta_{ei1}^2 \\
&+ \sum_{i=1}^{N}\sum_{j=1}^{N} a_{ij}(\lambda_{\max}(Z_i) + (\hat{d}_i - \breve{d}_i)\lambda_{\max}(U_i) \\
&+ \hat{d}_i^2 \lambda_{\max}(P_{3i}) + (\hat{d}_i - \breve{d}_i)^2 \lambda_{\max}(P_{4i}))\delta_{eij3}^2 \\
&+ \sum_{i=1}^{N} b_i(\frac{1}{2}\hat{d}_i^2 \lambda_{\max}(R_i))\delta_{ei2}^2 \\
&+ \sum_{i=1}^{N}\sum_{j=1}^{N} a_{ij}(\frac{1}{2}\hat{d}_i^2 \lambda_{\max}(Q_i))\delta_{eij4}^2.
\end{aligned}$$

REFERENCES

[1] X. Guan, B. Yang, C. Chen, W. Dai, and Y. Wang, "A comprehensive overview of cyber-physical systems: From perspective of feedback system," *IEEE/CAA J. Autom. Sinica*, vol. 3, no. 1, pp. 1–14, Jan. 2016.

[2] A. Ahmad, A. Paul, M. M. Rathore, and H. Chang, "Smart cyber society: Integration of capillary devices with high usability based on cyber–physical system," *Future Generat. Comput. Syst.*, vol. 56, no. 1, pp. 493–503, 2016.

[3] Z. Zheng, Z. Jin, L. Sun, and M. Zhu, "Adaptive sliding mode relative motion control for autonomous carrier landing of fixed-wing unmanned aerial vehicles," *IEEE Access*, vol. 5, no. 1, pp. 5556–5565, 2017.

[4] X. Xu, B. Cizmeci, C. Schuwerk, and E. Steinbach, "Model-mediated teleoperation: Toward stable and transparent teleoperation systems," *IEEE Access*, vol. 4, no. 1, pp. 425–449, 2016.

[5] R. Olfati-Saber and R. M. Murray, "Consensus problems in networks of agents with switching topology and time-delays," *IEEE Trans. Autom. Control*, vol. 49, no. 9, pp. 1520–1533, Sep. 2004.

[6] J. He, L. Duan, F. Hou, P. Cheng, and J. Chen, "Multiperiod scheduling for wireless sensor networks: A distributed consensus approach," *IEEE Trans. Signal Process.*, vol. 63, no. 7, pp. 1651–1663, Apr. 2015.

[7] C. Zhao, J. He, P. Cheng, and J. Chen, "Consensus-based energy management in smart grid with transmission losses and directed communication," *IEEE Trans. Smart Grid*, vol. 8, no. 5, pp. 2049–2061, Sep. 2017, doi: 10.1109/TSG.2015.2513772.

[8] E. Troja and S. Bakiras, "Optimizing privacy-preserving DSA for mobile clients," *Ad Hoc Netw.*, vol. 59, no. 1, pp. 71–85, 2017.

[9] R. Rakkiyappan, B. Kaviarasan, and J. H. Park, "Leader-following consensus for networked multi-teleoperator systems via stochastic sampled-data control," *Neurocomputing*, vol. 164, no. 1, pp. 272–280, 2015.

[10] A. Franchi, C. Masone, H. H. Bülthoff, and P. R. Giordano, "Bilateral teleoperation of multiple UAVs with decentralized bearing-only formation control," in *Proc. IEEE/RSJ Int. Conf. Intell. Robots Syst.*, Sep. 2011, pp. 2215–2222.

[11] X. Yang, C. Hua, J. Yan, and X. Guan, "New stability criteria for networked teleoperation system," *Inf. Sci.*, vol. 233, no. 1, pp. 244–254, 2013.

[12] U. Farooq, J. Gu, M. El-Hawary, M. U. Asad, and J. Luo, "An extended state convergence architecture for multilateral teleoperation systems," *IEEE Access*, vol. 5, no. 1, pp. 2063–2079, 2017.

[13] E. J. Rodriguez-Seda, J. J. Troy, C. A. Erignac, P. Murray, D. M. Stipanović, and M. W. Spong, "Bilateral teleoperation of multiple mobile agents: Coordinated motion and collision avoidance," *IEEE Trans. Control Syst. Technol.*, vol. 18, no. 4, pp. 984–992, Jul. 2010.

[14] T. Hu, Z. Lin, and B. M. Chen, "Analysis and design for discrete-time linear systems subject to actuator saturation," *Syst. Control Lett.*, vol. 45, no. 2, pp. 97–112, 2002.

[15] D. Zhai and Y. Xia, "Adaptive control for teleoperation system with varying time delays and input saturation constraints," *IEEE Trans. Ind. Electron.*, vol. 63, no. 11, pp. 6921–6929, Nov. 2016.

[16] C.-C. Hua, X. Yang, J, Yan, and X.-P. Guan, "On exploring the domain of attraction for bilateral teleoperator subject to interval delay and saturated P + d control scheme," *IEEE Trans. Autom. Control*, vol. 62, no. 6, pp. 2923–2928, Jun. 2017.

[17] F. Hashemzadeh, I. Hassanzadeh, and M. Tavakoli, "Teleoperation in the presence of varying time delays and sandwich linearity in actuators," *Automatica*, vol. 49, no. 9, pp. 2813–2821, 2013.

[18] J. Yan, Y. Wan, X. Luo, C. Chen, C. Hua, and X. Guan, "Formation control of teleoperating cyber-physical syste with time delay and actuator saturation," *IEEE Trans. Control Syst. Technol.* [Online]. Avaialble: http://ieeexplore.ieee.org/document/7947157/, doi: 10.1109/TCST.2017.2709266.2017.

[19] J. Yan, C.-L. Chen, X.-Y. Luo, X. Yang, C.-C. Hua, and X.-P. Guan, "Distributed formation control for teleoperating cyber-physical system under time delay and actuator saturation constrains," *Inf. Sci.*, vols. 370–371, no. 1, pp. 680–694, 2016.

[20] J. Yan, X. Luo, X. Yang, C. Hua, and X. Guan, "Consensus of multi-slave bilateral teleoperation system with time-varying delays," *J. Intell. Robot. Syst.*, vol. 76, no. 2, pp. 239–253, 2014.

[21] S. Sirouspour, "Modeling and control of cooperative teleoperation systems," *IEEE Trans. Robot.*, vol. 21, no. 6, pp. 1220–1225, Dec. 2005.

[22] J. Yan, X. Yang, C. Chen, X. Luo, and X. Guan, "Bilateral teleoperation of multiple agents with formation control," *IEEE/CAA J. Autom. Sinica*, vol. 1, no. 2, pp. 141–148, Apr. 2014.

[23] J. Yan, Y. Wan, C. Chen, C. Hua, and X. Guan, "Formation control of teleoperating cyber-physical system subject to time delay and actuator saturation constraints," in *Proc. 55th IEEE Conf. Decision Control*, Dec. 2016, pp. 4358–4363.

[24] A. Franchi, C. Secchi, H. I. Son, H. H. Bulthoff, and P. R. Giordano, "Bilateral teleoperation of groups of mobile robots with time-varying topology," *IEEE Trans. Robot.*, vol. 28, no. 5, pp. 1019–1033, Oct. 2012.

[25] R. Kelly, V. S. Davila, and A. Loria, *Control of Robot Manipulators in Joint Space*. London, U.K.: Springer, 2005.

[26] A. Seuret and F. Gouaisbaut, "Wirtinger-based integral inequality: Application to time-delay systems," *Automatica*, vol. 49, no. 9, pp. 2860–2866, Sep. 2013.

[27] C. D. Godsil and G. Royle, *Algebraic Graph Theory*. New York, NY, USA: Springer, 2001.

[28] A. Gasparri, R. Williams, A. Priolo, and G. Sukhatme, "Decentralized and parallel constructionsfor optimally rigid graphs in R^2," *IEEE Trans. Mobile Comput.*, vol. 14, no. 11, pp. 2216–2228, Nov. 2015.
[29] B. D. O. Anderson, C. Yu, and J. M. Hendrickx, "Rigid graph control architectures for autonomous formations," *IEEE Control Syst. Mag.*, vol. 28, no. 6, pp. 48–63, Dec. 2008.
[30] C. Yu and B. D. O. Anderson, "Development of redundant rigidity theory for formation control," *Int. J. Robust Nonlinear Control*, vol. 19, no. 13, pp. 1427–1446, 2008.
[31] S. Islam, P. X. Liu, J. Dias, and L. D. Seneviratne, "Adaptive control for robot manipulators using multiple parameter models," *Int. J. Control, Autom. Syst.*, vol. 14, no. 5, pp. 1365–1375, 2016.
[32] S. Islam, "State and impedance reflection based control interface for bilateral telerobotic system with asymmetric delay," *J. Intell. Robotic Syst.*, vol. 87, nos. 3–4, pp. 425–438, 2017, doi: 10.1007/s10846-017-0511-z.

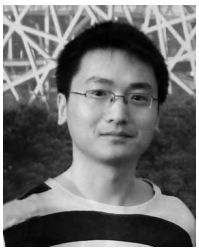

JING YAN received the B.Eng. degree in automation from Henan University, Kaifeng, China, in 2008, and the Ph.D. degree in control theory and control engineering from Yanshan University, Qinhuangdao, China, in 2014. In 2014, he was a Research Assistant with the Key Laboratory of System Control and Information Processing, Ministry of Education, Shanghai Jiaotong University, Shanghai, China. In 2016, he was a Research Associate with The University of Texas at Arlington, Arlington, USA. He is currently an Associate Professor with Yanshan University.

He has authored over 20 referred international journal and conference papers. He is the inventor of two patents. His research interests cover in networked teleoperation systems, underwater acoustic sensor networks, and cyberphysical systems. He was a recipient of the competitive National Graduate Scholarship from the Ministry of Education of China in 2012. He received the Excellence Paper Award from the National Doctoral Academic Forum of System Control and Information Processing in 2012, and the Science and Technology Innovation Award from Yanshan University in 2013.

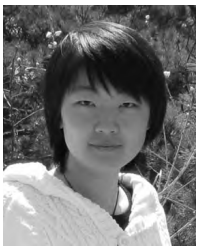

XIAN YANG received the B.S. degree in automation and the Ph.D. degree in control theory and control engineering from Yanshan University, Qinhuangdao, China, in 2010 and 2014, respectively. She is currently an Associate Professor with Yanshan University.

She has authored over 20 referred international journal and conference papers. She is the inventor of two patents. Her research interests cover in networked teleoperation systems, underwater cyberphysical systems, and nonlinear control. She was a recipient of the competitive National Graduate Scholarship from the Ministry of Education of China in 2013, 2014, and 2015.

XIAOYUAN LUO received the Ph.D. degree from the School of Electrical Engineering, Yanshan University, Qinhuangdao, China, in 2005. He is currently a Professor with Yanshan University.

His research interests include multiagent cooperation control, security of cyber-physical systems, and control of intelligent transportation systems.

CAILIAN CHEN received the B.Eng. and M.Eng. degrees in automatic control from Yanshan University, China, in 2000 and 2002, respectively, and the Ph.D. degree in control and systems from the City University of Hong Kong, Hong Kong, in 2006. She joined the Department of Automation, Shanghai Jiao Tong University, in 2008, as an Associate Professor, where she is currently a Full Professor.

She has authored and/or co-authored two research monographs and over 100 referred international journal and conference papers. She is the inventor of over 20 patents. Her research interests include wireless sensor and actuator network and application in industrial automation, vehicular networks and application in intelligent transportation systems, and estimation and control for multiagent systems. She received the IEEE TRANSACTIONS ON FUZZY SYSTEMS Outstanding Paper Award in 2008. She was one of the First Prize Winners of the Natural Science Award from the Ministry of Education of China in 2006 and 2016, respectively. She was honored as a Changjiang Young Scholar by the Ministry of Education of China in 2015 and the Excellent Young Researcher by NSF of China in 2016.

XINPING GUAN was the Professor and the Dean of Electrical Engineering, Yanshan University, China. He is currently the Chair Professor with Shanghai Jiao Tong University, China, where he is also the Deputy Director of the University Research Management Office, and the Director of the Key Laboratory of Systems Control and Information Processing, Ministry of Education, China.

He has authored and/or co-authored four research monographs, over 270 papers in IEEE Transactions and other peer-reviewed journals, and numerous conference papers. He has finished/been working on many national key projects as a Principal Investigator. He is the Leader of the prestigious Innovative Research Team of the National Natural Science Foundation of China. His current research interests include industrial cyber-physical systems, wireless networking and applications in smart city and smart factory, and underwater sensor networks. He is an Executive Committee Member of the Chinese Automation Association Council and the Chinese Artificial Intelligence Association Council. He received the First Prize of Natural Science Award from the Ministry of Education of China in 2006 and 2016, respectively, and the Second Prize of the National Natural Science Award of China in 2008. He was a recipient of the IEEE TRANSACTIONS ON FUZZY SYSTEMS Outstanding Paper Award in 2008. He is a National Outstanding Youth honored by NSF of China, a Changjiang Scholar by the Ministry of Education of China, and the State-level Scholar of New Century Bai Qianwan Talent Program of China.